

DISSERTATION

QUANTIFYING THE EFFECTS OF PEDIATRIC OBESITY ON MUSCULOSKELETAL
FUNCTION AND BIOMECHANICAL LOADING DURING WALKING

Submitted by

Zachary F. Lerner

Graduate Degree Program in Bioengineering

In partial fulfillment of the requirements

For the Degree of Doctor of Philosophy

Colorado State University

Fort Collins, Colorado

Spring 2015

Doctoral Committee:

Advisor: Raymond Browning

Bradley Davidson

Tammy Donahue

Christian Puttlitz

Raoul Reiser

Copyright by Zachary Forest Lerner 2015

All Rights Reserved

ABSTRACT

QUANTIFYING THE EFFECTS OF PEDIATRIC OBESITY ON MUSCULOSKELETAL FUNCTION AND BIOMECHANICAL LOADING DURING WALKING

With the high prevalence of pediatric obesity worldwide, there is a critical need for structured physical activity interventions during childhood. However, obese children exhibit altered walking mechanics that are associated with decreased gait stability, reduced walking performance and an increased prevalence of musculoskeletal pain and pathology. Left unaddressed, the increased pain and orthopedic conditions associated with pediatric obesity may lead to reduced physical activity and a cycle of perpetual weight gain for the child and future adult. To enhance the efficacy of health and weight loss interventions, clinicians could benefit from an improved understanding of how pediatric obesity affects the neuromuscular and musculoskeletal systems during walking, the most common form of daily activity.

The mechanisms for the altered gait and associated risks to the developing musculoskeletal system in obese children are not well understood, particularly as they relate to excess adiposity and exercise related fatigue. This void in the literature may be attributed in part to the lack of experimental and computational tools necessary to accurately quantify muscle function and joint loads during walking in obese and healthy-weight adults and children. Therefore, to improve our understanding of the musculoskeletal mechanisms for the altered gait mechanics and orthopedic disorders exhibited by obese children, this dissertation sought to first, establish the proper methods to adequately quantify the necessary biomechanical measures in

obese and healthy-weight individuals, and second, determine the effects of obesity and duration on muscle function and tibiofemoral loading during walking in children.

The accuracy of muscle and joint contact forces estimated from dynamic musculoskeletal simulations is dependent upon the experimental kinematic data used as inputs. Subcutaneous adipose tissue makes the measurement of representative kinematics from motion analysis particularly challenging in overweight and obese individuals. We developed an obesity-specific kinematic marker set and methodology that accounted for subcutaneous adiposity. Next, we determined how this methodology affected muscle and joint contact forces predicted from musculoskeletal simulations of walking in obese individuals. The marker set methodology had a significant effect on model quantified lower-extremity kinematics, muscle forces, and hip and knee joint contact forces. We demonstrated the need for biomechanists to account for subcutaneous adiposity during kinematic data collection and proposed a feasible solution that likely improves the accuracy of musculoskeletal simulations in overweight and obese people.

Understanding orthopedic disorders of biological and prosthetic knee joints requires knowledge of the *in-vivo* loading environment during activities of daily living. Anthropometric and orthopedic differences between individuals make accurate predictions from generic musculoskeletal models a challenge. We developed a knee mechanism within a full-body OpenSim musculoskeletal model that incorporated subject-specific knee parameters to predict medial and lateral tibiofemoral contact forces. To assess the accuracy of our model, we compared measured to predicted medial and lateral compartment contact forces during walking in an individual with an instrumented knee replacement. We determined the importance of specifying subject-specific tibiofemoral alignment and contact locations and validated a simple approach to measure and specify these parameters on a subject-specific basis using radiography.

The biomechanical mechanisms responsible for the altered gait mechanics in obese children are not well understood. We investigated the relationship between adiposity and lower extremity kinematics, muscle force requirements, and individual muscle contributions to whole body dynamics by generating musculoskeletal simulations of walking in a group of children with a range of adiposity. Body fat percentage was correlated with average knee flexion angle during stance and pelvic obliquity range of motion, as well as with relative vasti, gluteus medius and soleus force production. The functional demands and relative force requirements of the hip abductors during walking in pediatric obesity likely contribute to the altered gait mechanics in obese children.

The combination of larger magnitude and altered application of tibiofemoral loads during physical activity in obese children is commonly theorized to contribute to their increased risk of orthopedic disorders of the knee, such as growth-plate suppression leading to conditions of malalignment. To evaluate this theory and determine how prolonged activity affects knee loading, we quantified the effects of pediatric obesity and walking duration on medial and lateral tibiofemoral contact forces. We found that obese children have elevated medial compartment magnitudes, loading rates, and load share, which further increased with walking duration. The altered tibiofemoral loading environment during walking in obese children likely contributes to their increased risk of knee pain and pathology. These risks may increase with activity duration.

This dissertation provides a foundation for improved understanding of the effects of pediatric obesity on the neuromuscular and musculoskeletal systems during walking. The main research outcomes from this dissertation aim to improve rehabilitation and activity guidelines that minimize the risk of musculoskeletal pain and pathology in obese children, address degenerative gait mechanics, and assist in breaking the cycle of weight gain.

ACKNOWLEDGEMENTS

First and foremost, I would like to thank my advisor, Ray Browning, for guiding me through my doctoral research, and for whom I have the utmost gratitude and appreciation. Beyond providing excellent advice on the mechanics of conducting research, Ray has taught me how to enjoy the “process” of research, ask interesting and impactful questions, and celebrate successes, small and large. Ray’s eternal enthusiasm for our work made it easy to stay motivated and productive. My career and future accomplishments will forever be influenced by his brilliant mentorship.

I would like to thank each member of my PhD committee, which includes Bradley Davidson, Tammy Donahue, Christian Puttlitz, and Raoul Reiser, for their guidance and challenging yet supportive feedback.

I would also like to express my gratitude towards the many researchers and collaborators that I have had the privilege of working with during my time as a PhD student. In particular, I want to thank Wayne Board for his help and assistance in experimental data collection; Scott Delp and Matthew DeMers for their guidance in musculoskeletal modeling; Christian Puttlitz and Ben Gadowski for the opportunity to learn additional experimental methods and techniques; Sarah Shultz for providing a valuable source of experimental data; and last, but not least, all of my fellow lab members for making my time in the lab enjoyable and productive.

Finally, I thank the National Institute of Child Health & Human Development and the American College of Sports Medicine for providing funding through pre-doctoral fellowships. Their support made this research possible, and I am honored to be a recipient of both fellowship awards.

TABLE OF CONTENTS

ABSTRACT.....	ii
ACKNOWLEDGEMENTS.....	v
LIST OF TABLES.....	viii
LIST OF FIGURES.....	ix
1. INTRODUCTION.....	1
1.1 Research Focus.....	1
1.2 Dissertation Overview.....	3
1.3 Significance of this Work.....	4
2. DEVELOPMENT AND ANALYSIS OF AN EXPERIMENTAL KINEMATIC METHODOLOGY FOR USE IN OBESE INDIVIDUALS.....	6
2.1 Chapter Overview.....	6
2.2 Introduction.....	7
2.3 Methods.....	9
2.4 Results.....	14
2.5 Discussion.....	18
2.6 Conclusion.....	22
3. DEVELOPMENT OF A COMPUTATIONAL MODEL TO ACCURATELY PREDICT MEDIAL AND LATERAL TIBIOFEMORAL CONTACT FORCES.....	24
3.1 Chapter Overview.....	24
3.2 Introduction.....	25
3.3 Methods.....	27

3.4 Results.....	34
3.5 Discussion.....	38
3.6 Conclusion	42
4. HOW PEDIATRIC OBESITY AFFECTS MUSCLE FUNCTION DURING WALKING ..	43
4.1 Chapter Overview	43
4.2 Introduction.....	44
4.3 Methods.....	46
4.4 Results.....	51
4.5 Discussion.....	55
4.6 Conclusion	61
5. HOW PEDIATRIC OBESITY AFFECTS MEDIAL AND LATERAL TIBIOFEMORAL CONTACT FORCES DURING WALKING.....	63
5.1 Chapter Overview	63
5.2 Introduction.....	64
5.3 Methods.....	66
5.4 Results.....	73
5.5 Discussion.....	78
5.6 Conclusion	81
6. CONCLUSION.....	83
6.1 Dissertation Summary.....	83
6.2 Future Work	84
REFERENCES	87

LIST OF TABLES

Table 2.1	15
Table 3.1	37
Table 4.1	47
Table 4.2	55
Table 4.3	55
Table 5.1	66

LIST OF FIGURES

Figure 1.1	1
Figure 2.1	11
Figure 2.2	12
Figure 2.3	16
Figure 2.4	17
Figure 2.5	18
Figure 3.1	28
Figure 3.2	30
Figure 3.3	30
Figure 3.4	35
Figure 3.5	36
Figure 3.6	38
Figure 4.1	52
Figure 4.2	53
Figure 4.3	54
Figure 4.4	58
Figure 4.5	58
Figure 5.1	67
Figure 5.2	70
Figure 5.3	74
Figure 5.4	75

Figure 5.5 76

Figure 5.6 77

1. INTRODUCTION

1.1 Research Focus

Pediatric obesity is a major and growing global public health concern. There is a critical need for structured physical activity interventions during childhood. However, obese children exhibit altered walking mechanics that have been associated with an increased prevalence of musculoskeletal pain and pathology [1]. Left unaddressed, the increased pain and orthopedic conditions associated with pediatric obesity can lead to reduced physical activity and may facilitate a cycle of perpetual weight gain (Figure 1.1) [2]. To improve exercise prescription, clinicians could benefit from an improved understanding of how pediatric obesity affects the neuromuscular and musculoskeletal systems during walking.

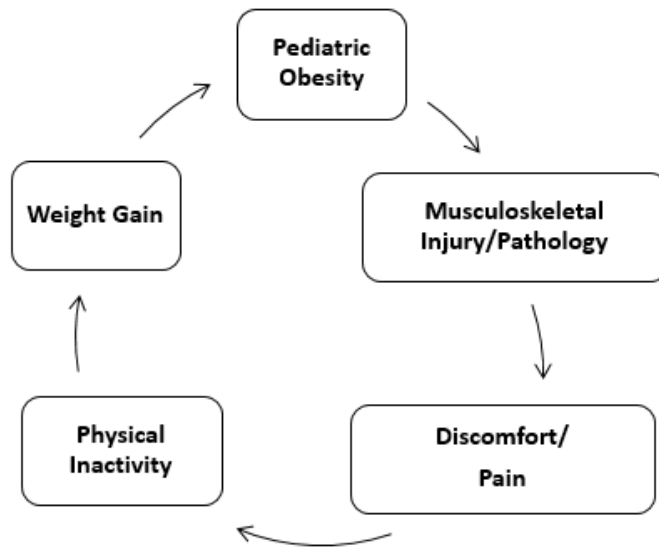


Figure 1.1 The cycle of weight gain theorized in pediatric obesity.

There are three reasons why the literature is incomplete in regards to adequately describing the effects of pediatric obesity on the neuromuscular and musculoskeletal systems during walking. First, experimental data collection methods have not adequately accounted for subcutaneous adiposity, particularly around the pelvis and torso, which obscures the motion of the underlying skeleton. This experimental oversight has resulted in inconclusive and conflicting results in the literature [3-6]. Second, rather than reporting individual muscle forces and joint contact forces, prior studies have only reported joint angles, moments, and powers during walking in obese and healthy-weight children [4-6]. Therefore, we lack information on how pediatric obesity affects individual muscle function and the magnitudes, distributions, and loading rates of the joint contact forces. Finally, prior studies may lack real-world applicability because experimental protocols have not reflected how children engage in daily physically activity. These studies report biomechanical outcome measures during walking only several steps rather than during walking continuously for several minutes [4-6]. Due to these limitations and the collective void in the literature, clinicians are unable to appropriately weigh the risk-benefit ratio of increased physical activity on the short and long-term health of the growing musculoskeletal system in obese children.

The primary purpose of this dissertation was to investigate how pediatric obesity affects muscle function and knee joint loading during walking. While gait analysis and musculoskeletal modeling tools have made large improvements in recent years, two methodological challenges remained. The first challenge was that predictions of muscle and joint forces from dynamic simulations rely on accurately quantifying experimental motions of the skeleton, which is obscured by adiposity in obese individuals. The second challenge was that existing computational methods used to predict tibiofemoral contact forces were unsuitable for studying

how pediatric obesity affects tibiofemoral compartment (i.e. medial and lateral) loads during walking. Therefore, this dissertation had four goals. The first goal of this dissertation was to develop a kinematic marker set/methodology suitable for use in obese individuals that accounted for subcutaneous adiposity, and to determine the effect of using such a methodology to estimate muscle and joint contact forces during walking. The second goal of this dissertation was to develop an experimental protocol and musculoskeletal model that addressed subject-specific tibiofemoral alignment and contact locations and computed medial and lateral compartment contact forces during walking. The third goal of this dissertation was to investigate the relationship between adiposity and lower extremity kinematics, muscle force requirements, and individual muscle contributions to whole body dynamics during walking. Finally, the fourth goal of this dissertation was to determine the effects of pediatric obesity and walking duration on medial and lateral tibiofemoral contact forces.

1.2 Dissertation Overview

This dissertation is organized around four individual research studies, each designed to meet one of the dissertation's four goals. Each study is either published or under review as an original research article in a scientific journal. Following this introduction, Chapters 2 and 3 describe the development of the experimental and computational tools necessary for studying the proposed research on muscle function and joint loading during walking in children. Chapter 2, published in *Medicine and Science in Sport and Exercise* [7], explores an experimental methodology that was developed to more accurately capture kinematic data in obese individuals, while Chapter 3, published in *Journal of Biomechanics* [8], presents the development and validation of a combined experimental and computational approach to accurately predict medial and lateral tibiofemoral compartment contact forces during walking. Chapters 4 and 5 apply the

methodological advancements presented in the two preceding chapters to investigate how pediatric obesity affects muscle function and knee joint loading during walking. In particular, Chapter 4, published in *Journal of Biomechanics* [9], examines how adiposity affects individual muscle forces and their contributions to mass center accelerations during walking, and Chapter 5, under review in *Medicine and Science in Sport and Exercise*, examines how pediatric obesity and walking duration affects the magnitude, distribution, and loading rates of medial and lateral tibiofemoral compartment contact forces. The sixth and final chapter summarizes the major findings of the four research studies and identifies several areas of future research.

1.3 Significance of this Work

This dissertation sought to investigate the impact of pediatric obesity on musculoskeletal function during walking, which, due to the global increase in childhood obesity and the associated comorbidities, has both clinical and public health implications. Because of the challenges associated with accurately quantifying the necessary musculoskeletal outcome measures in obese children, this investigation required the development of novel experimental and computational biomechanics/biomedical engineering tools. Therefore, this dissertation has implications for both the biomechanics and clinical research communities.

The first two research studies of this dissertation make contributions primarily to the biomechanics community. The main contribution from Chapter 2 was the development and analysis of a kinematic marker set suitable for accurately quantifying the motion of the skeleton despite subcutaneous adiposity. This study, which demonstrated the importance of accounting for subcutaneous adiposity on estimates of muscle and joint contact forces, provides the biomechanics community with a readily achievable approach for use in gait analysis of obese individuals. The main contribution from Chapter 3 was the development of a customizable knee

joint mechanism within a full-body OpenSim gait model that was able to resolve individual tibiofemoral compartment contact forces. We developed and validated an experimental protocol to estimate the subject-specific parameters necessary to accurately resolve medial and lateral tibiofemoral contact forces during walking. We have made this musculoskeletal model publically available at www.simtk.org/home/med-lat-knee/.

The final two research studies of this dissertation make contributions primarily to the clinical research community. The main contribution from Chapter 4 was an improved understanding of how adiposity affects individual muscle function during walking in children. Obese children walk differently than healthy-weight children, but the neuromuscular reasons are not well understood. We created dynamic musculoskeletal simulations of gait to identify the muscles that are implicated in the altered gait mechanics exhibited by obese children. This knowledge can be used to prescribe activities and/or strength training that may facilitate improved quality of movement. The main contribution from Chapter 5 was an improved understanding of the effects of pediatric obesity and walking duration on medial and lateral tibiofemoral compartment contact forces. With regard to caloric balance and cardiovascular health, obese children may benefit from increased physical activity. However, altered tibiofemoral loading during physical activity in obese children likely contribute to their increased risk of orthopedic disorders of the knee. We found that obese children walk with greater medial compartment contact forces, loading rates, and load share, providing empirical evidence for the reported orthopedic conditions. Further, we found that these measures of medial compartment loading increased with duration, suggesting that the prescription of shorter activity durations may reduce musculoskeletal injury risk for obese children.

2. DEVELOPMENT AND ANALYSIS OF AN EXPERIMENTAL KINEMATIC METHODOLOGY FOR USE IN OBESE INDIVIDUALS¹

2.1 Chapter Overview

The accuracy of muscle and joint contact forces estimated from dynamic musculoskeletal simulations are dependent upon the experimental kinematic data used as inputs. Subcutaneous adipose tissue makes the measurement of representative kinematics from motion analysis particularly challenging in overweight and obese individuals. The purpose of this study was to develop an obesity-specific kinematic marker set/methodology that accounted for subcutaneous adiposity, and to determine the effect of using such a methodology to estimate muscle and joint contact forces in moderately obese adults. Experimental kinematic data from both the obesity-specific methodology, which utilized digitized markers and marker clusters, and a modified Helen Hayes marker methodology were used to generate musculoskeletal simulations of walking in obese and nonobese adults. Good agreement was found in lower-extremity kinematics, muscle forces, and hip and knee joint contact forces between the two marker set methodologies in the nonobese participants, demonstrating the ability for the obesity-specific marker set/methodology to replicate lower extremity kinematics. In the obese group, marker set methodology had a

¹ The contents of this chapter have been published in:

Medicine and Science in Sports and Exercise (2014); 46(6): 1261-1267

Zachary F. Lerner
Wayne J. Board
Raymond C. Browning

significant effect on lower-extremity kinematics, muscle forces, and hip and knee joint contact forces, with the Helen Hayes marker set methodology yielding larger muscle and first peak hip and knee contact forces compared to the estimates derived when using the obesity-specific marker set/methodology. This study demonstrates the need for biomechanists to account for subcutaneous adiposity during kinematic data collection, and proposes a feasible solution that may improve the accuracy of musculoskeletal simulations in overweight and obese people.

2.2 Introduction

Accurate estimates of muscle and joint contact forces from dynamic simulations of human locomotion provide critical insight into normal and pathological function of the musculoskeletal system [10-14]. For example, musculoskeletal simulations can be used to enhance our understanding of the biomechanical mechanisms linking obesity and large joint osteoarthritis. The accuracy of experimentally driven musculoskeletal simulations is dependent upon the ability to collect accurate kinematic data. Using passive reflective markers placed on the surface of the skin to determine the kinematics of the underlying skeleton can result in inaccurate marker placement and soft tissue artifact (STA), particularly in overweight and obese subjects [15]. As our population becomes progressively overweight and obese [16], participants in locomotor biomechanics studies, especially those using obese participants, will likely include individuals with substantial subcutaneous adiposity. The majority of studies that use motion capture for gait analysis, even those directly assessing obesity [17-19], use standard kinematic marker sets/methodologies developed for nonobese individuals that do not attempt to account for adiposity, namely, some version of the Helen Hayes marker set methodology [20].

Inaccurate marker placement and STA can lead to gross errors in basic biomechanical measures, such as hip and knee joint kinematics and net muscle moments [21]. Additionally,

when a generic musculoskeletal model is scaled to the anthropometrics of a subject, using markers placed on the skin to represent the size and motion of the underlying skeleton of an overweight or obese individual may lead to inaccurate scale factors and marker trajectories, respectively. Although various methods have been proposed to account for excess soft tissue obscuring the underlying bone, such as lateral relocation of the anterior superior iliac spines (ASIS) markers [22], DEXA derived anthropometric measures [22-24], biplane fluoroscopy [25], and functional joint locating methods [26], they are not consistently used and are limited by effectiveness, practicality, and/or cost. A methodology to account for excess soft tissue in overweight and obese individuals that is relatively accurate, relatively simple and inexpensive to employ would aid researchers who conduct biomechanical analyses of obese individuals [27]. In addition, investigating the influence of marker set methodology on musculoskeletal simulation outputs will provide insights into the sensitivity of kinematics and muscle/joint forces to how the musculoskeletal system is modeled.

The purpose of this study was three-fold: first, to develop an obesity-specific motion capture methodology that was easy to implement and accounted for subcutaneous adiposity; second, to demonstrate the ability of the new methodology to replicate the kinematics of nonobese individuals using a standard methodology, and third, to determine the effect of using a methodology specifically developed for obese individuals to estimate muscle (vasti, hamstring, rectus femoris, and iliopsoas) and axial hip and knee contact forces during walking in obese adults. We hypothesized that 1) there would not be significant differences in lower extremity joint angles, lower extremity muscle forces, and axial hip and knee joint contact forces between the obesity-specific methodology and a modified Helen Hayes methodology in nonobese

individuals, but 2) there would be significant differences in these same parameters between the methodologies in obese individuals.

2.3 Methods

Subjects

Nine obese adults with a body mass index (BMI) of 35.0 (3.78) $\text{kg}\cdot\text{m}^{-2}$ (Mean (SD)), of which 8 were female, and 9 nonobese adults with a BMI of 22.1 (1.02) $\text{kg}\cdot\text{m}^{-2}$, of which 5 were female, in good health with no known acute/chronic diseases or limitations to physical activity, participated in our study. All subjects gave written informed consent approved by Colorado State University's Human Research Institutional Review Board.

Experimental Protocol

As part of a larger study, participants walked at nine randomized speed grade combinations, ranging from 0.50 $\text{m}\cdot\text{s}^{-1}$ to 1.75 $\text{m}\cdot\text{s}^{-1}$ at grades ranging from 0-9°. The biomechanics data was collected for the last 30 seconds of the 6 minute trials, and there were 5 minutes of rest between trials. For purposes of this study, we used data from the 1.25 $\text{m}\cdot\text{s}^{-1}$, level (0°) trials.

Experimental Data

Ground reaction forces were collected using a dual-belt, force measuring treadmill (Fully Instrumented Treadmill; Bertec Corp, Columbus, OH) recording at 1000 Hz, while kinematics were collected using a 10-camera motion capture system (Nexus, Vicon, Centennial, CO) recording at 100 Hz. Marker trajectory and GRF data were digitally low-pass filtered at 5 Hz and 12 Hz, respectively, using fourth-order zero-lag Butterworth filters. Electromyographic (EMG) data (Noraxon, Scottsdale, Arizona) from bipolar surface electrodes recording at 1000 Hz was collected for the soleus, lateral gastrocnemius, vastus lateralis, vastus medialis, biceps femoris

long head, and semimembranosus muscles using standard procedures [28]. The EMG signal was band-pass filtered (16-380 Hz), fully rectified and finally low-pass filtered at 7 Hz.

Kinematic Marker Sets

The obesity-specific methodology was developed for use in obese individuals and consisted of a combination of physical reflective markers, marker clusters, and digitally defined markers (Figure 2.1, Figure 2.2). Reflective markers were placed over the following anatomical landmarks identified via palpation: 7th cervical vertebrae, acromion processes, right scapular inferior angle, sterno-clavicular notch, xyphoid process, 10th thoracic vertebrae, posterior-superior iliac spines (PSIS), ASIS, iliac crests (IC), medial and lateral epicondyles of the femurs, medial and lateral malleoli, calcanei, first metatarsal heads, second metatarsal heads, and proximal and distal heads of the 5th metatarsals. Marker clusters (four non-collinear markers affixed to a rigid plate) were adhered to the thighs, shanks, and sacrum to aid in three-dimensional tracking. A spring-loaded digitizing pointer (C-Motion, Germantown, MD) was used to digitally mark the ASIS and IC. We placed the tip of the digitizing pointer on the soft tissue directly over the anatomical landmark and depressed the digitizing pointer until it reached the underlying bone in order to mark the location for post-processing. This process was also used to define the location of the digital ASIS and IC landmarks relative to three markers on the sacral cluster using Visual 3D (C-Motion/Visual 3D, Germantown, MD). This relationship was used during the motion trials to calculate the digital ASIS and IC trajectories during post processing in Visual 3D. Coordinate data (i.e. marker trajectories) for all additional markers were determined in Visual 3D as well. A modified Helen Hayes (basic) methodology [20] was defined as a subset of the previously described passive reflective markers as follows: five markers on the torso (excluding the acromion processes), ASIS, PSIS, one marker from each thigh cluster (posterior-

superior marker), the lateral condyles of the femur, one marker from each shank cluster (posterior-superior marker), the lateral malleoli, the calcanei, and second metatarsal heads.

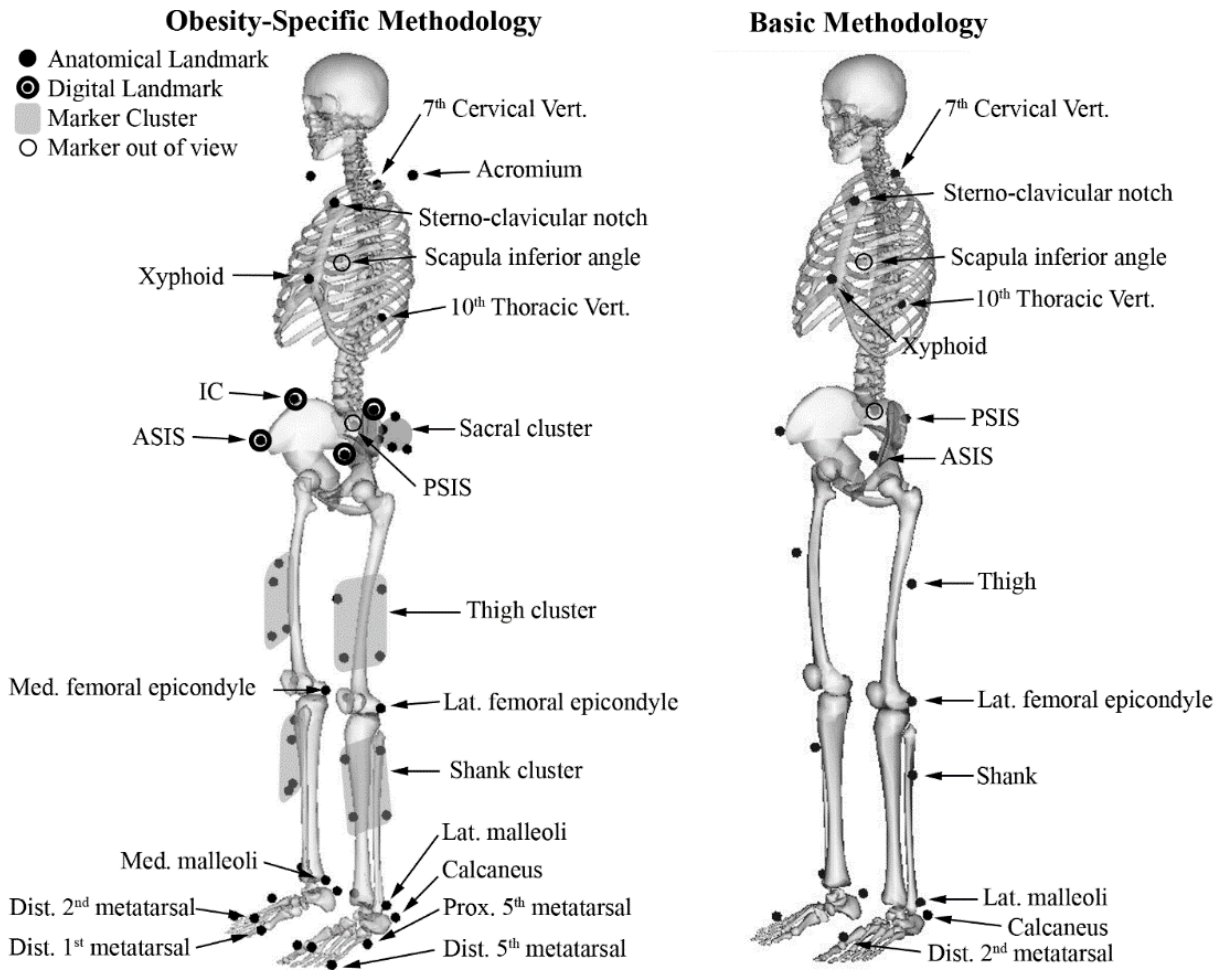


Figure 2.1 Marker placements of the obesity-specific methodology and the subset of markers comprising the basic methodology relative to skeletal landmarks.



Figure 2.2 Marker and marker cluster placements of the obesity-specific methodology on a representative subject.

Dynamic Musculoskeletal Simulation

For each obese participant and for each methodology, we used OpenSim to scale a generic musculoskeletal model, determine joint angles, and quantify muscle and joint contact forces [29]. The OpenSim model was comprised of 12 body segments with 19 degrees of freedom, 92 muscle-tendon actuators, and a knee joint that included a planar patellofemoral joint that articulated with the femur [10, 30, 31]. The distance between the experimental ASIS markers (i.e. inter-ASIS distance between physical ASIS markers in the case of the basic methodology, or digitized ASIS markers in the case of the obesity-specific methodology) were used to uniformly scale the pelvis of each subject specific musculoskeletal model. The distance between the experimental ASIS and lateral femoral epicondyle markers were used to scale each thigh segment, while the distance between lateral femoral epicondyle and lateral malleoli markers were used to scale each shank segment. The joint angles during each gait trial were calculated using OpenSim's inverse kinematics analysis with standard marker weighting factors

used to generate joint angles in nonobese individuals that follow guidelines from gait analysis software including Visual 3D, Vicon, and OpenSim [12, 29]. We used a weighted static optimization approach to resolve individual muscle forces from the net joint torques determined through the method of inverse dynamics [12, 29]. The static optimization objective function minimized the sum of squared muscle activations while incorporating individual muscle weighting constants of seven for the gastrocnemius, three for the hamstrings and one for all other muscles in the model. These weighting constants, established by Steele et al., resulted in the best agreement between model estimated tibiofemoral forces and those measured experimentally from an instrumented knee joint replacement [12, 29, 32]. Residual actuators were applied to the pelvis during static optimization to account for dynamic inconsistencies resulting from modeling assumptions and small errors in the experimental data. OpenSim's Joint Reaction analysis was used to determine joint contact forces [12, 29], which represent the forces and moments that each joint structure carries due to all muscle forces, external loads, and inertial loads of the model. The compressive knee contact force was computed as the component of the resultant force acting on the tibia and parallel to the long axis of the tibia, while the compressive hip contact force was computed as the component of the resultant force acting on the femoral head, parallel to the long axis of the femur.

Joint kinematics (sagittal plane joint angles of the pelvis, hip and knee), muscle forces (vasti, hamstring, rectus femoris, and iliopsoas), and axial joint contact forces (hip and knee) are reported from the right leg, normalized and averaged across two representative gait cycles per subject, and then averaged across subjects for each methodology. Muscle forces and axial knee joint contact forces were normalized to the body weight (BW) of each subject.

Statistical analysis

Student's *t*-tests were used to determine if there were significant differences in kinematic and kinetic variables (averages, maximums, and/or minimums) between the basic and obesity-specific methodologies within each group. A criterion of $p < 0.05$ defined significance. SigmaPlot version 11.0 (Systat Software, Inc., San Jose, CA) was used to perform the statistical analyses.

2.4 Results

We present the results of eight obese individuals, as Static Optimization failed, despite repeated attempts, to find a solution using the basic methodology for one obese participant. The mean residual force in each coordinate direction applied to the center of mass of the pelvis was less than 4.1% BW for each completed simulation. In the nonobese participants, joint angles, muscle forces, and first peak hip and knee joint contact forces were not significantly different between the basic and obesity-specific methodologies (Table 2.1). In the obese individuals, peak hip flexion during stance and pelvic tilt angles were significantly different between the kinematic marker set methodologies (Figure 2.3). First peak rectus femoris muscle forces were significantly smaller (0.27 BW vs. 0.73 BW, $p < 0.001$) in the obesity-specific methodology vs. the basic methodology, while all other muscle forces were similar. A qualitative comparison between estimated muscle forces and experimental EMG revealed relatively good agreement for the activation timing of the vasti and biceps femoris long head muscles (Figure 2.4). Compared to the basic methodology, the obesity-specific methodology resulted in smaller first peak axial hip (2.82 BW vs. 3.58 BW, $p = 0.002$), and knee (2.12 BW vs. 2.54 BW, $p = 0.021$) contact forces (Figure 2.5).

Table 2.1 Differences in joint angles, peak muscle forces, and joint contact forces (JCF) between the obesity-specific methodology relative to the basic methodology for the obese and nonobese participants. * Denotes significant differences within each group across marker set methodologies. Mean differences for each variable were found by subtracting the quantity obtained using the basic methodology from the quantity obtained using the obesity-specific methodology.

	Mean Difference Between Sets	
	Obese	Nonobese
Average Anterior Pelvic Tilt (°)	-13.3*	-0.6
Peak Hip Flexion during Stance (°)	-10.0*	1.3
Peak Knee Flexion during Stance (°)	-1.4	-0.6
Vasti Force (BW)	-0.12	<0.01
Hamstring Force (BW)	-0.08	<0.01
Rectus Force (BW)	-0.46*	-0.14
Iliopsoas Force (BW)	-0.36	-0.29
1 st Peak Hip JCF (BW)	-0.76*	-0.02
1 st Peak Knee JCF (BW)	-0.43*	-0.12

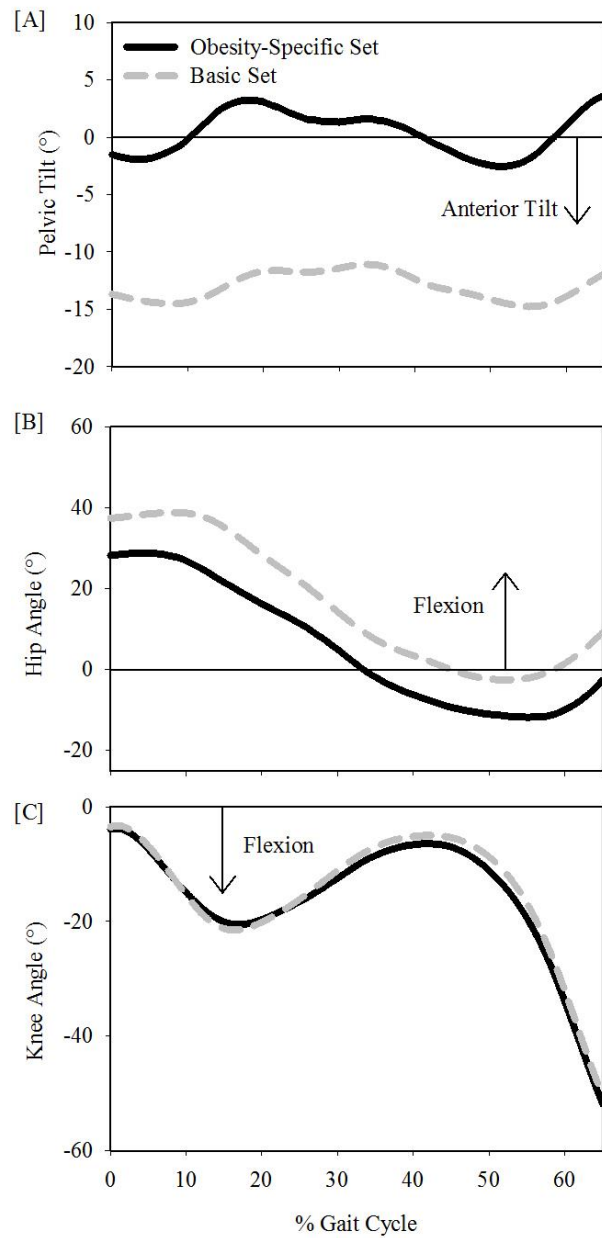


Figure 2.3 Sagittal plane pelvic (top panel), hip (middle panel), and knee (bottom panel) joint angles in obese individuals determined using the obesity-specific (black solid line) and basic (grey dashed line) methodologies. Hip flexion angle and anterior pelvic tilt were significantly greater in the basic vs. obesity-specific methodologies.

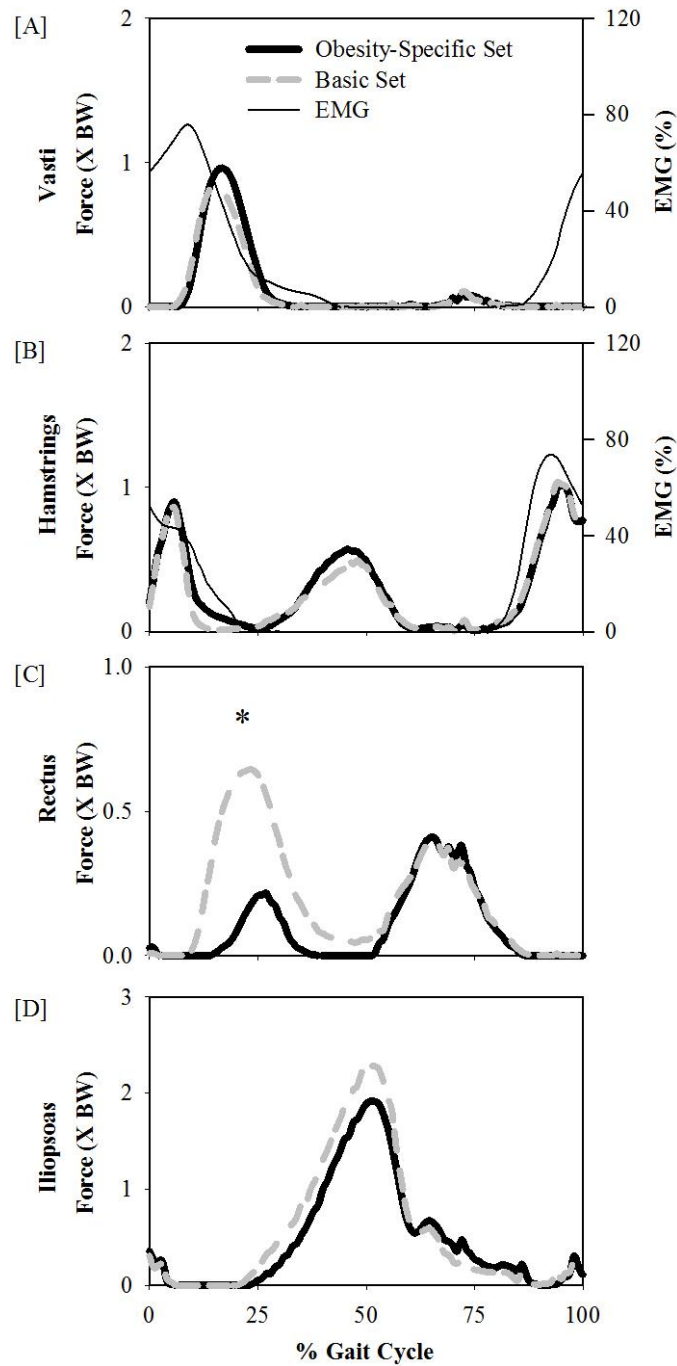


Figure 2.4 Body weight normalized muscle forces in obese individuals, estimated using the obesity-specific methodology (black solid line) and the basic methodology (dashed grey line). * Denotes significant differences across marker set methodologies. Vasti and biceps femoris long head EMG was included in the first and second panels, respectively. Vasti (1st panel), hamstring (2nd panel), and iliopsoas (4th panel) BW normalized muscle forces were similar between methodologies, while the rectus femoris (3rd panel) muscle had greater BW normalized force output in the basic vs. the obesity-specific methodology. The stance phase occurs during ~0-60% of the gait cycle.

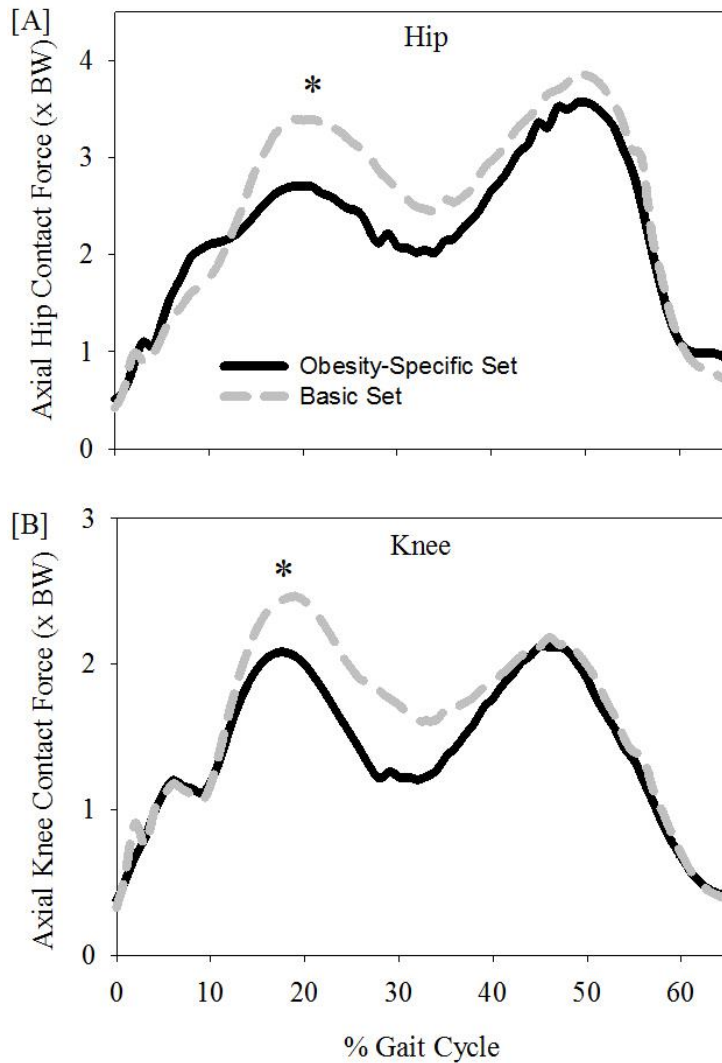


Figure 2.5 Body weight normalized axial hip (top panel) and knee (bottom panel) contact forces in obese individuals, estimated using the obesity-specific methodology (black solid line) and the basic methodology (dashed grey line). * Denotes significant differences across marker set methodologies. First peak hip and knee contact forces were significantly greater in the basic vs. the obesity specific methodologies.

2.5 Discussion

We accept our first hypothesis that sagittal plane joint angles, muscle forces, and joint contact forces would be similar between the methodologies in nonobese individuals. This demonstrates the ability of the obesity-specific methodology to replicate lower extremity kinematics determined from the well-established, modified Helen Hayes methodology. We found significant differences in hip flexion and pelvic tilt joint angles, rectus femoris muscle forces and

first peak axial hip and knee joint contact forces between marker methodologies in the obese group, and therefore also accept our second hypothesis.

To account for additional subcutaneous adipose tissue at the pelvis and lower extremities in overweight and obese versus nonobese individuals, we created an obesity-specific methodology by probing and digitally marking several key pelvic landmarks directly on the underlying bone and adding additional marker clusters. As reported in the literature, but not in this current evaluation, segment tracking in the frontal and transverse planes is likely more accurate when utilizing marker clusters [33]. We elected to define the location and trajectory of the ASIS and IC digital markers relative to a cluster placed on the sacrum because the sacrum moves in unison with the pelvis, has reduced subcutaneous adipose tissue, and is likely to be less susceptible to STA than other locations on the pelvis.

During the musculoskeletal model scaling process, it is *possible* to adjust the location of the model's virtual markers relative to the skeleton to reduce the error in relation to the experimental markers. However, to be accurate this method requires some knowledge of the actual location of the skeleton (e.g. via an MRI image) relative to the skin and may be prone to inaccuracy when used to adjust markers by many centimeters, as required in obese individuals. Additionally, merely measuring the depth of the soft tissue separating a marker placed on the skin and the bone, and adjusting the virtual marker in the model accordingly, may not be adequate at the pelvis because physical markers attached on the abdomen in obese experience substantial STA and tend to move with the torso rather than the pelvis. Using a digitizing pointer to provide a physical measure of the location of underlying bony landmarks, and defining those digital locations relative to skeletal landmarks less susceptible to STA is likely more accurate and repeatable.

There was substantial subcutaneous abdominal adiposity positioned between the ASIS markers placed on the skin and the actual ASIS bony landmarks on the bone in all of the obese subjects. This made it difficult to accurately track the underlying pelvic skeleton when the basic methodology was used to generate joint angles. The inverse kinematics analysis, which solves the least squares equation for all of the markers, resulted in a kinematic solution that caused significant anterior rotation (anterior pelvic tilt) of the pelvis in the basic methodology. This is because musculoskeletal models capable of estimating muscle and joint forces are fully constrained, and a translation, as opposed to a rotation, of the pelvis to reduce the pelvic region marker errors would increase the marker errors on the body segments down the kinematic chain (i.e. the thigh and shank). We systematically tested a range of pelvic region marker weighting factors, yet the significant rotation of the pelvis remained when the adipose tissue was not accounted for (i.e. the basic methodology). Due to the kinematic relationship between the pelvis and femur, a more anterior rotated pelvis will increase the hip flexion angle even if the femur has not changed its own global orientation. Thus, the basic methodology resulted in likely inaccurate pelvic tilt and hip flexion angles.

It was surprising that sagittal plane knee joint angles were similar between methodologies in the obese individuals because, while we did not expect differences in the sagittal plane orientation of the shank and foot, we did expect differences in the sagittal plane orientation of the femur. However, as mentioned previously, this is due to how the inverse kinematic solution of a fully constrained musculoskeletal model accounts for inaccurate marker placements around the pelvis (i.e. a preference to modulate the orientation of the pelvis rather than the hip joint center location).

With similar vasti and hamstring forces during early stance between the methodologies in the obese group, it was initially counter intuitive to find significantly different axial knee joint contact forces. On closer inspection, however, because the basic methodology elicited greater rectus femoris force output there was a net increase in the axial knee contact force during early stance vs. the obesity-specific methodology. During mid-late stance, axial knee joint contact forces were not significantly different between methodologies because the force outputs from the muscles crossing the knee joint were generally similar during that portion of the gait cycle.

The first peak axial hip and knee contact forces estimated using the obesity-specific methodology (hip: 2.82 BW, knee: 2.12 BW) were in closer agreement to values reported in the literature from instrumented implants at similar walking speeds and in a similar population (hip: ~2.75 BW [34], knee: ~2.15 BW [35]), than those estimated from the basic methodology (hip: 3.58 BW, knee: 2.54 BW). Heller et al. compared model estimated and experimentally measured in-vivo hip contact forces and reported a tendency for musculoskeletal simulations to overestimate forces at that joint [34]. Interestingly, they used a kinematic marker set, similar to the basic marker set used in this study, comprised solely of passive reflective markers affixed to the skin even though half of their subjects were overweight ($\text{BMI} > 25 \text{ kg}\cdot\text{m}^{-2}$), while the other half was obese ($\text{BMI} > 30 \text{ kg}\cdot\text{m}^{-2}$). Our results demonstrate that failing to account for soft tissue at the pelvis may result in artificially large force output from certain hip flexor muscles, which might explain the tendency for their simulations to overestimate hip contact forces in this population.

The primary limitation of this study was the small sample size, yet we believe our primary goal to establish the importance of accounting for adipose tissue during kinematic data collection was demonstrated, nevertheless. Surface EMG has been shown to be a viable way to

measure muscle activity in the lower extremity of obese adults [36]; however, the effectiveness of this method in this population can be limited and must be regarded as a limitation. Another limitation of this study was that scaling of each model's pelvis segment based on the digital ASIS locations did not directly account for the overlying mass of adipose tissue. However, it has been reported that body mass distributions are generally similar between obese and nonobese adults [37] and the inertial properties of the body segments likely have limited influence on model kinetics during the stance phase of gait [38]. Thus, uniform scaling of the inertial properties in obese adults should have limited impact on the presented results. A subsequent limitation of this study was that we used a weighted static optimization approach to indirectly validate muscle force estimates based on comparing estimated and experimentally measured contact forces at the knee joint alone. However, we are confident in the ability of these Static Optimization weighting factors to provide reasonable estimates of both hip and knee contact forces because much of the primary hip musculature (i.e. rectus femoris, biceps femoris long head, semimembranosus, semitendinosus, and sartorius) cross both the hip and knee joints and were accounted for in the knee joint validation. Additionally, we have found that relative differences between conditions (e.g. marker set methodologies or weight status) are insensitive to the Static Optimization weighting factors themselves. Finally, results from inverse kinematic and inverse dynamic analyses generated using unconstrained (i.e. 6 degree of freedom) models common to gait analysis software such as Vicon and Visual 3D were not included in this study but warrant further investigation.

2.6 Conclusion

In summary, the effect of marker set methodology on estimates of muscle forces and axial hip and knee joint contact forces in obese individuals was significant, with the basic

methodology yielding larger muscle and joint contact forces. There were no significant differences in these same measures between the methodologies in the nonobese participants. The measured differences between the two methodologies can likely be attributed to tracking the motion of the pelvis using the digital ASIS and IC marker locations in the case of the obesity-specific methodology, vs. the physical ASIS and IC markers placed on the skin in the case of the basic methodology. These findings are not only relevant for studies directly assessing the biomechanics of obese individuals, but also for studies in which a subset of the subjects are overweight or obese, because applying a basic methodology to all of the subjects, or different methodologies to separate subject groups, may act as confounding factors. The results of this study support the need for biomechanists to adopt kinematic data collection protocols that accounts for adipose tissue in overweight and obese individuals.

3. DEVELOPMENT OF A COMPUTATIONAL MODEL TO ACCURATELY PREDICT MEDIAL AND LATERAL TIBIOFEMORAL CONTACT FORCES²

3.1 Chapter Overview

Understanding degeneration of biological and prosthetic knee joints requires knowledge of the *in-vivo* loading environment during activities of daily living. Musculoskeletal models can estimate medial/lateral tibiofemoral compartment contact forces, yet anthropometric differences between individuals make accurate predictions challenging. We developed a full-body OpenSim musculoskeletal model with a knee joint that incorporates subject-specific tibiofemoral alignment (i.e. knee varus-valgus) and geometry (i.e. contact locations). We tested the accuracy of our model and determined the importance of these subject-specific parameters by comparing estimated to measured medial and lateral contact forces during walking in an individual with an instrumented knee replacement and post-operative genu valgum (6°). The errors in the predictions of the first peak medial and lateral contact force were 12.4% and 11.9%, respectively, for a model with subject-specific tibiofemoral alignment and contact locations determined via radiographic analysis, vs. 63.1% and 42.0%, respectively, for a model with generic parameters. We found that each degree of tibiofemoral alignment deviation altered the first peak medial

² The contents of this chapter have been published in:

Journal of Biomechanics (2015); 48(4): 644-650

Zachary F. Lerner
Matthew S. DeMers
Scott L. Delp
Raymond C. Browning

compartment contact force by 51N ($r^2=0.99$), while each millimeter of medial-lateral translation of the compartment contact point locations altered the first peak medial compartment contact force by 41N ($r^2=0.99$). The model, available at www.simtk.org/home/med-lat-knee/, enables the specification of subject-specific joint alignment and compartment contact locations to more accurately estimate medial and lateral tibiofemoral contact forces in individuals with non-neutral alignment.

3.2 Introduction

Abnormal knee loads are implicated in tibiofemoral osteoarthritis [39], which affects more than 12% of US adults [40]. The distribution of tibiofemoral contact forces between the medial and lateral compartments can be influenced by frontal-plane tibiofemoral alignment and affect degeneration of biological [41] and prosthetic [42] knees. The treatment of orthopedic disorders of the knee is likely to benefit from an improved understanding of the *in-vivo* knee loading environment during activities of daily living.

Musculoskeletal models allow researchers to investigate medial/lateral tibiofemoral contact forces during activities like walking [32, 43]. Some modeling approaches require complex, multi-step analyses, or the use of both full-body gait models and finite element or contact models [44-48]. Finite element and contact models rely on an accurate representation of the articulating joint surfaces and require imaging techniques that may be unavailable or prohibitively expensive. Resolving the magnitudes of medial/lateral forces by approximating medial/lateral compartment points of contact is a promising approach for estimating contact forces [49-51]; however, no open-source, full-body gait model contains knee joint definitions that allow direct computation of medial/lateral contact forces.

Predictions of medial/lateral tibiofemoral contact forces in an individual using a musculoskeletal model with generic geometry may be inaccurate when the model does not accurately represent the individual. The specification of certain subject-specific model parameters may improve accuracy [50]. Two parameters, frontal-plane tibiofemoral alignment and medial/lateral compartment contact locations, are likely to influence model-predicted medial/lateral compartment contact forces by altering how muscle forces and external loads pass relative to each compartment. Frontal-plane tibiofemoral alignment affects loading of the knee [47, 52-54], and can vary up to $\pm 3.75^\circ$ in individuals without obvious genu valgum-varum [55]. Existing modeling approaches have limitations that hinder the accurate representation of a subject's frontal-plane alignment; for example, generic models typically lack or constrain the frontal-plane motion of the knee [44, 49-51] and subject-specific models based on geometry determined from MRI or CT images are of non-weight-bearing limbs [46, 50]. In addition, when medial/lateral compartment contact is approximated through single points, the locations of these points influence how the tibiofemoral loads are distributed. It has been assumed that the medial/lateral compartment contact locations are centered at the midline of the femoral condyles [51] in biological knees or located at set distances from the joint center in prosthetic knees [50], but variability in alignment and joint degeneration may alter these locations.

To address the need to calculate tibiofemoral loads accurately this study had three goals. The first was to develop a musculoskeletal model that accounts for differences in tibiofemoral alignment and contact locations and computes medial/lateral contact forces during walking. The second goal was to quantify the accuracy of knee contact force estimates made using generic geometry and subject-specific geometry by comparing these estimates to *in-vivo* measurements from an individual with an instrumented knee replacement and genu valgum. The third goal was

to evaluate the effects of model-specified frontal-plane knee alignment and contact point locations on medial/lateral contact force predictions. The model, experimental data, and contact force predictions are freely available at www.simtk.org.

3.3 Methods

Model Development

To compute medial and lateral tibiofemoral contact forces during walking we developed a model of the tibiofemoral joint in OpenSim [10] and incorporated it within a published full body musculoskeletal model [56]. The published model, designed for studying gait, was comprised of 18 body segments and 92 muscle-tendon actuators. Model degrees of freedom (DOF) included a ball-and-socket joint between the third and fourth lumbar vertebra, 3 translations and 3 rotations of the pelvis, a ball-and-socket joint at each hip, and revolute ankle and subtalar joints. In our model, the sagittal plane rotation and translations of the tibia and patella relative to the femur were identical to those specified by (Delp et al, 1990); however, we augmented the mechanism defining the tibiofemoral kinematics.

The tibiofemoral model introduced components for configuring frontal-plane alignment of the knee and for resolving distinct medial and lateral tibiofemoral forces. We introduced a distal femoral component body and a tibial plateau body (represented by CAD geometry of the instrumented implant, Figure 3.1, pink) with orientation parameters for configuring frontal-plane alignment in the femur (θ_1) and tibia (θ_2). Between the femoral component and the tibial plateau, we defined a series of joints to characterize the tibiofemoral kinematics and medial/lateral load distribution. Firstly, the knee joint from Delp et al. (1990) defined the sagittal-plane rotations and translations of the knee between the femoral component and the sagittal articulation frame of reference (Figure 3.1A, hidden, Figure 3.1B, translucent). Secondly, two revolute joints

connected the sagittal articulation frame to medial and lateral tibiofemoral compartments (Figure 3.1, purple). The axes for these two revolute joints were perpendicular to the frontal-plane. Lastly, the medial and lateral compartments were welded at the anteroposterior mid-point of the tibial plateaus such that they remained fixed to the tibia while articulating with the surface of the femoral component during flexion-extension. The patella segment articulated with the femoral-condyle segment according to [56]. The quadriceps muscles wrapped around the patella before attaching to the tibial tuberosity to redirect the quadriceps forces along the line of action of the patellar ligament and allow the resultant tibiofemoral contact forces to be computed [56].

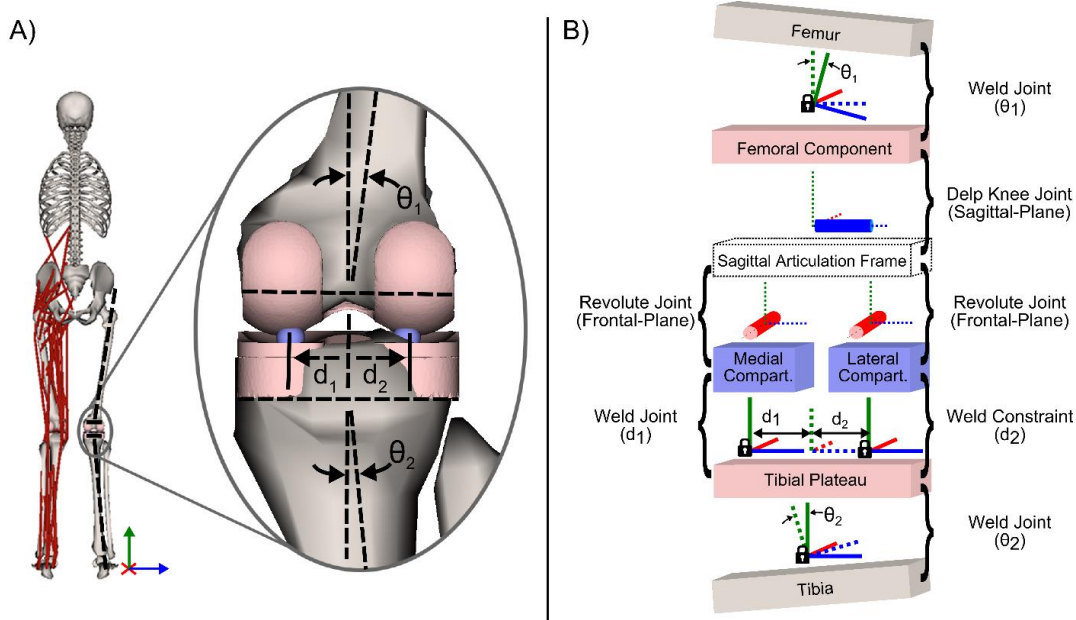


Figure 3.1 Graphical (A) and schematic (B) depictions of the medial/lateral compartment joint structures in our musculoskeletal model. In both the graphic and schematic, the red axis is perpendicular to the frontal-plane, the green axis is perpendicular to the transverse-plane, and the blue axis is perpendicular to the sagittal-plane. The “Delp Knee Joint” defines the sagittal-plane tibiofemoral translations and rotations specified by [31] (blue cylinder in B). Two revolute joints (red cylinders), acting in the frontal-plane, connect the sagittal articulation frame (translucent) to both the medial and lateral compartments (purple). By acting in parallel, these two revolute joints share all loads transmitted between the femur and tibia and resolve the medial and lateral contact forces required to balance the net reaction forces and frontal-plane moments across the tibiofemoral joint. The medial compartment is fixed to the tibial plateau with a weld joint, and the lateral compartment is fixed to the tibial plateau with a weld constraint (black locks). Correspondingly, the knee remained a single DOF joint with articulation only in the sagittal plane. The locations of the medial and lateral compartments can be specified on a subject-specific basis (d_1 and d_2 in the inset graphic and schematic). Similarly, the model’s tibiofemoral alignment can be specified (θ_1 and θ_2 in the inset graphic and schematic) by modifying the weld joint between the femur and femoral component and the weld joint between the tibial plateau and tibia.

Experimental Data

We used experimental data from a subject with an instrumented knee replacement (right knee, male, age 83, mass 67 kg, height 1.72 m) to generate dynamic simulations of walking. These data have been made available by the Knee Load Grand Challenge [32]. Researchers collected kinematic, kinetic, and instrumented implant data simultaneously during over-ground walking. Validated regression equations were used to calculate separate medial and lateral tibiofemoral compartment contact forces from the instrumented knee joint [57].

Established methods [55] were used to quantify the frontal-plane alignment of the subject's right lower-extremity from a standing anteroposterior radiograph (Figure 3.2). The angle formed between the intersection of the mechanical axes of the femur and tibia was used to specify subject-specific model alignment. To model lower-extremity alignment, θ_1 and θ_2 from Figure 3.1 are each specified as one half of the varus-valgus alignment angle ($180^\circ - \theta$ from Figure 3.2). To estimate subject-specific medial/lateral compartment contact locations, we measured the distance between the centerline of the femoral implant component and the centerline of the tibial implant component using a higher resolution anteroposterior radiograph of the knee (Figure 3.3). A measurement scale was established from the known width of the implant. Contact model predictions using *in-vivo* measurements of a similar implant have indicated an intercondylar distance of 40mm [58], and this distance has been used previously to inform model contact points [50]. Therefore, we maintained this intercondylar distance while shifting the medial/lateral contact locations medially by the distance (d) measured from the radiograph.



Figure 3.2 Anteroposterior radiograph of the participant's lower-extremity used to determine the subject-specific alignment for the musculoskeletal model. Angle θ (174°) was found by drawing lines connecting the hip, knee, and ankle joint centers, which were defined as the center of the femoral head, center of the femoral condyles, and midpoint of the medial and lateral margins of the ankle, respectively.

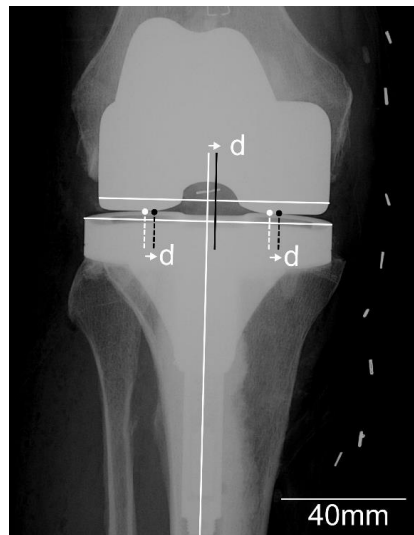


Figure 3.3 The anteroposterior radiograph of the participant's instrumented (right) knee that was used to determine the frontal-plane location of the femoral implant component relative to the tibial implant component. The parameter, d , was measured as the distance between the centerlines of each component (3mm). A measurement scale was set from the known width of the implant. In the model, we specified the subject-specific medial/lateral compartment contact locations (black dots) by shifting the generic medial/lateral locations (white dots) medially by d , thus maintaining an intercondylar distance of the instrumented implant. Therefore, for the fully-informed model and contact-point-informed model, the medial compartment point of contact was located 23mm medial of the knee joint center, while the lateral compartment point of contact was located 17mm lateral of the knee joint center.

Varying Tibiofemoral Specificity in the Musculoskeletal Model

To isolate the effects of specifying each subject-specific parameter we conducted simulations with the following four conditions of our musculoskeletal model.

Fully-Informed Model: This model had subject-specific tibiofemoral alignment ($\theta=174^\circ$) and contact locations informed via radiographic analysis. Medial compartment contact was located 23mm medial of the knee joint center and lateral compartment contact was located 17mm lateral of the knee joint center.

Uninformed Model: Based on data from an instrumented implant contact model for a neutrally aligned lower-extremity [58], and matching assumptions for an artificial knee implant made previously [50], we specified the generic frontal-plane locations of the medial/lateral compartment structures 20mm medial and lateral of the knee joint center. The tibiofemoral alignment for this model ($\theta=180^\circ$) was maintained from skeletal geometry originally defined by [31].

Alignment-Informed Model: This model had subject-specific alignment ($\theta=174^\circ$) but uninformed contact locations (20mm medial and lateral of the joint center).

Contact-Point-Informed Model: This model had subject-specific contact locations (medial compartment: 23mm medial of the joint center, lateral compartment: 17mm lateral of the joint center) but uninformed alignment ($\theta=180^\circ$).

To investigate the effects of model-specified tibiofemoral alignment on model-predictions, we created contact-point-informed models with variable tibiofemoral alignment ranging from 0° - 8° valgus, at 2° increments. To investigate the effects of model-specified medial/lateral compartment contact locations on model-predictions, we created alignment-

informed models with variable medial/lateral contact point locations spanning reported translations ($\pm 4\text{mm}$) at 2mm increments with 40mm inter-condylar distances.

Musculoskeletal Simulation of Walking

We used marker location data from anatomical landmarks collected during a standing calibration trial to scale our models in OpenSim. For each scaled model, we used OpenSim's inverse kinematics analysis, which minimized the errors between markers fixed to the model and experimentally measured marker trajectories [10], to determine the joint angles during four over-ground walking trials. Model kinematics were recalculated for every model condition while the ground reaction forces remained the same. Because muscle forces are the main determinant of compressive tibiofemoral contact forces [59], variations in muscle activity greatly influence the magnitude and accuracy of knee joint contact force predictions [56]. We resolved individual muscle forces using a weighted static optimization approach that was calibrated to the subject [12, 29]. The objective function minimized the sum of squared muscle activations while incorporating individual muscle weighting values using the method described by [12]. We manually adjusted the weighting values by half-integers until the combined first and second peak error between the measured and predicted medial/lateral tibiofemoral contact force was minimized for this subject. Muscle weighting factors of 1.5 for the gastrocnemius, 2 for the hamstrings, and 1 for all other muscles in the model, resulted in the lowest combined medial/lateral first and second peak prediction errors for each of the model conditions. The same weighting factors were used across all model conditions.

We computed the forces in the medial/lateral compartment joint structures using OpenSim's JointReaction analyses [12], which determines the resultant forces and moments acting on each articulating joint structure from all muscle forces and external and internal loads

applied to the model. Medial/lateral tibiofemoral contact forces were computed as the component of each resultant force acting normal to the tibial plateau.

We used the fully-informed model to verify the contact forces predicted by the medial/lateral joint structures by comparing the outputs from the JointReaction analysis to the medial/lateral contact forces determined from the well-established point-contact method [51]. This method balances the forces and moments acting at the knee joint about medial/lateral tibiofemoral contact points based on the principle of static equilibrium. OpenSim's inverse dynamics tool was used to determine the external abduction-adduction moment, while the muscle analysis tool was used to determine individual muscle moment arms about the medial and lateral compartment joint structures. The contact forces acting on the medial/lateral joint structures of our OpenSim model, as reported from the JointReaction analysis, were identical to the medial/lateral tibiofemoral contact forces quantified using the point-contact method.

Statistical Analysis

For each model condition, the contact force predictions for each walking trial were normalized to percent stance phase and averaged across stance phases to determine the mean and standard deviation. We calculated 95% confidence intervals to determine if statistically significant differences existed for first and second peak contact forces between model predictions and the *in-vivo* measurements, and to determine if significant differences existed between peak muscle forces. Regression analysis was used to determine the relationship between model-specified tibiofemoral alignment and contact point locations and first peak medial compartment forces. We also calculated the total (medial+lateral) root-mean-square errors (RMSE) between the predicted and measured contact forces. SigmaPlot, version 11.0 (Systat Software, Inc., San Jose, CA) was used to perform the statistical analyses.

3.4 Results

The fully-informed model had the best prediction accuracy. The alignment-informed model resulted in more accurate predictions than the contact-point-informed model; the least accurate was the uniformed model (Figure 3.4, Figure 3.5). Specifying subject-specific alignment and contact locations improved prediction accuracy by decreasing the contact force in the medial compartment and increasing the contact force in the lateral compartment (Figure 3.4). Compared to the uniformed model, first peak prediction accuracy increased by 51% in the medial compartment and 30% in the lateral compartment when the fully-informed model was used (Figure 3.5).

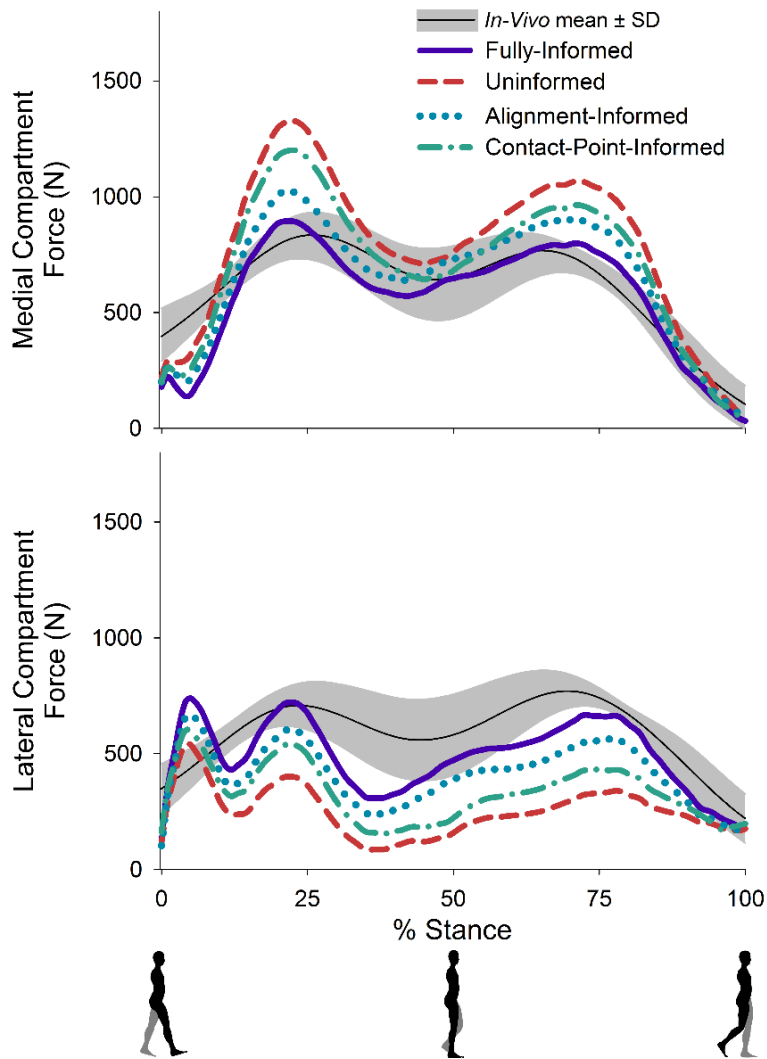


Figure 3.4 Medial (top) and lateral (bottom) compartment tibiofemoral contact forces during stance measured *in-vivo* from the instrumented implant (skinny black line) and predicted using the fully-informed (purple, solid line), uninformed (red, dashed line), alignment-informed (blue, dotted line), and contact-point-informed (green, dash-dot line) models.

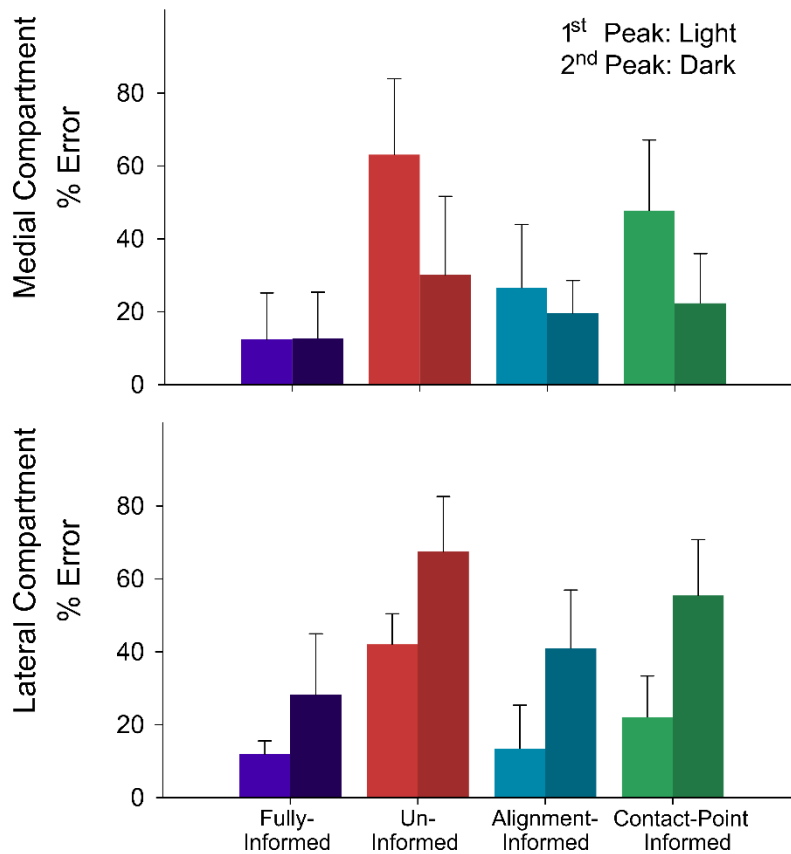


Figure 3.5 Percent error in first (light) and second (dark) peak medial (top) and lateral (bottom) tibiofemoral contact forces between the *in-vivo* measurements from the instrumented implant and the fully-informed (purple), uninformed (red), alignment-informed (blue), and contact-point-informed (green) models. Error bars represent 1 standard deviation (SD).

The contact force predictions from the fully-informed model were statistically similar to the *in-vivo* measurements for each peak in both the medial and lateral compartments; predictions from the uninformed model were only statistically similar for the second peak in the medial compartment (Table 3.1). Over the stance phase, predictions from the fully-informed, uninformed, alignment-informed, and contact-point-informed models had RMSE of 220N, 332N, 241N, and 297N, respectively.

Table 3.1 95% Confidence Intervals (CI) of the medial and lateral compartment first and second peak contact forces for the *in-vivo* data measured from the instrumented implant and each model condition. Bolded entries denote 95% CIs for the model predictions that do not overlap with the 95% CI for the *in-vivo* data (indicating significant difference).

	First Peak (N)		Second Peak (N)	
	Medial	Lateral	Medial	Lateral
<i>In-Vivo</i>	679-991	556-871	695-871	657-911
Fully-Informed	827-1002	635-825	559-987	399-714
Uniformed	1234-1461	319-502	786-1244	85-417
Alignment-Informed	951-1139	531-689	648-1095	302-612
Contact-Point-Informed	1119-1322	439-663	703-1136	183-507

Specifying a more valgus alignment decreased medial compartment force and increased lateral compartment force (Figure 3.6). Specifying a medial shift of the contact locations had the same effect. We found that each additional degree of tibiofemoral valgus alignment decreased the first peak of the medial contact force by 51N and increased the first peak of the lateral contact force by 30N ($r^2=0.99$). Translating the contact point locations medially by 1mm decreased the first peak of the medial contact force by 41N and increased the first peak of the lateral compartment contact force by 33N ($r^2=0.99$); translating the contact point locations laterally by 1mm had the opposite effect.

Muscle forces were the primary contributor to the knee joint contact force. For the fully-informed model, the sum of the muscle forces crossing the knee was 903N at the first peak of knee loading and 853N at the second peak. The sum of the muscle forces crossing the knee were not significantly different between model conditions. Individual peak muscle forces were similar between model conditions for all muscles except for the tensor-fasciae-latae, which increased from 62N in the uniformed model condition to 82N in the alignment-informed and fully-informed model conditions.

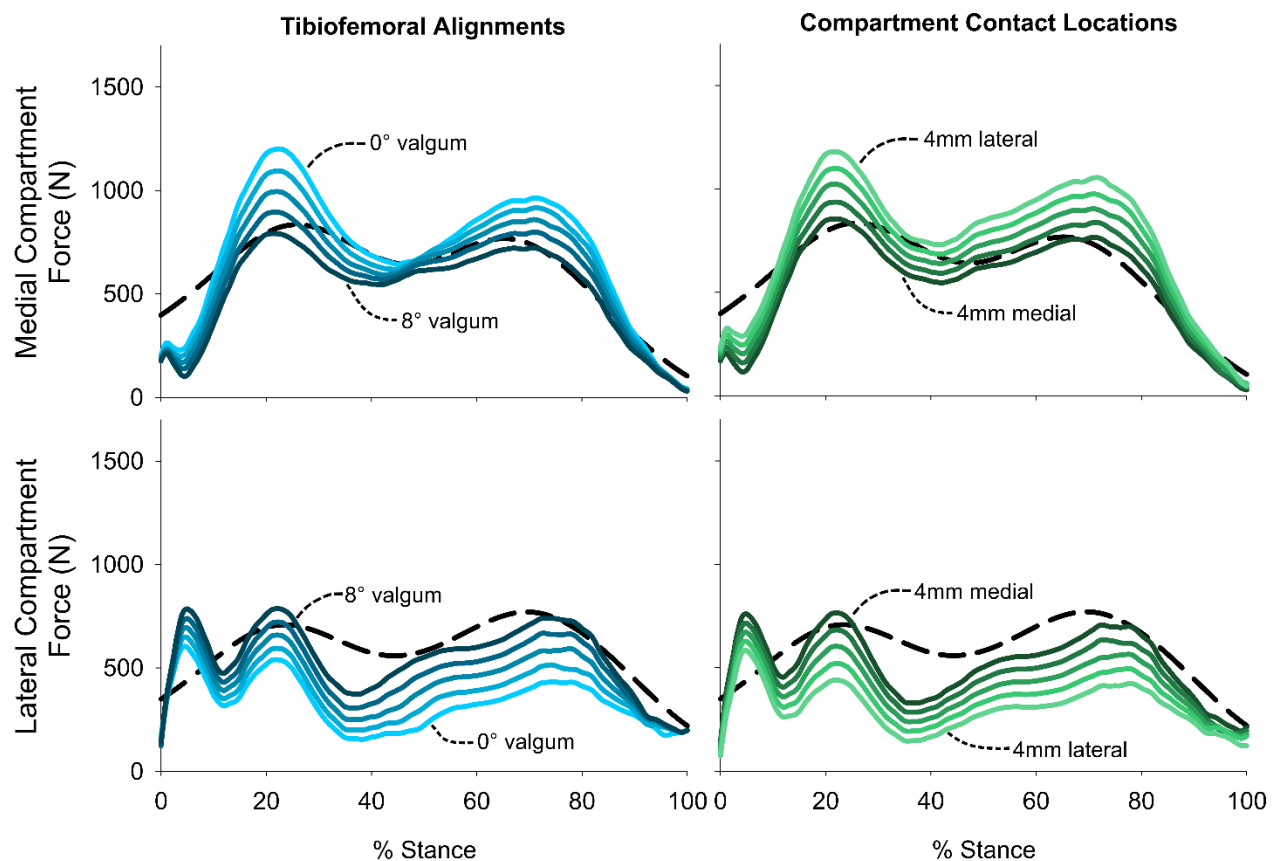


Figure 3.6 Effects of model-specified alignment (left), and compartment contact locations (right) on medial compartment (top) and lateral compartment (bottom) tibiofemoral contact forces during stance. The black-dashed lines represent the *in-vivo* measurements. Deviation of model-specified tibiofemoral alignment from 8° genu valgum (dark blue) to generic alignment (0° genu valgum, light blue), at 2° increments. Deviation of compartment contact locations from 4mm medial (dark green) to 4mm lateral (light green), at 2mm increments.

3.5 Discussion

We developed a novel, configurable knee joint in a full body musculoskeletal model that simplifies the prediction of medial/lateral tibiofemoral contact forces during locomotion, fulfilling the first goal of this study. This model allows investigators to specify subject-specific joint alignment and compartment contact locations to more accurately estimate tibiofemoral contact forces in individuals with non-neutral alignment.

The second goal of this study was to quantify the prediction accuracy of knee contact forces in an individual with non-neutral tibiofemoral alignment using our model with generic

geometric parameters versus our model with subject-specific parameters. We found that prediction accuracy was improved by specifying each subject-specific parameter. However, predictions for all model conditions had limited accuracy during early stance (Figure 3.4). Since muscles crossing the knee are not producing relatively large forces during this interval (e.g. summed muscle forces were <405N at 10% of stance), the predictions appear sensitive to small errors in the frontal-plane application of the external forces. During mid-stance, the lateral contact force was under-predicted for all models. Our objective function, which minimizes muscle activation and produces low levels of muscle co-contraction, may contribute to the reduced mid-stance accuracy since significant levels of co-contraction has been reported in older adults during mid-stance [60]. Furthermore, we selected static optimization weighting factors that minimized the first and second peak error, but not mid-stance error. Therefore, our results were not optimized for this portion of the gait cycle.

The third goal of this study was to investigate how geometric parameters, in particular tibiofemoral alignment and contact locations, affect estimates of medial/lateral contact forces. Our results indicate that frontal-plane tibiofemoral alignment is an important model parameter when predicting medial/lateral compartment contact forces. Hast et al. predicted medial/lateral contact forces from the same subject and dataset used in our study, but did not report incorporating subject-specific frontal-plane alignment [44]. Acknowledging that they used a different approach to estimate muscle and contact forces, they reported larger medial contact forces and smaller lateral contact forces compared to the *in-vivo* data. Their results resemble our predictions from our model with neutral alignment. Specifying subject-specific tibiofemoral alignment may therefore improve estimates of medial/lateral contact forces from other approaches that rely on knee models with a constrained abduction-adduction DOF. Thelen et al.

report that small variations in tibiofemoral alignment ($\pm 2^\circ$) in their dynamic contact model altered the medial-lateral distribution by up to 12% [48], suggesting that specification of subject-specific alignment would be important in this type of model as well.

Predictions of medial/lateral tibiofemoral contact forces were directly proportional to model-specified frontal-plane alignment (Figure 3.6). This relationship is supported by findings from a study with five individuals with instrumented knee implants and a range of post-operative lower-extremity alignments [53]. Thirty percent of total knee replacement cases result in postoperative alignment beyond $\pm 3^\circ$ varus-valgus [61], while the standard deviations of tibiofemoral alignment are 3° in healthy individuals and 8° in osteoarthritic individuals [62]. A 3° difference between model and subject alignment would alter first peak medial contact force predictions by 23% of body-weight and lateral contact force predictions by 14% of body-weight. Researchers can likely improve contact force estimates by utilizing subject-specific knee alignment acquired from radiographic images.

Our model resolved medial/lateral compartment loads by approximating them as though they occurred at single points of contact. We estimated these contact locations from an anteroposterior knee radiograph with knowledge of the intercondylar distance (40mm) determined from a similar implant [58]. Since a non-neutral lower-extremity may influence the relative placement of the femoral and tibial prosthesis components, we analyzed a radiograph of the subject's instrumented knee. We found a medial shift of the femoral component relative to the tibial component. Therefore, we shifted the medial/lateral locations in our model accordingly, while maintaining the previously reported intercondylar distance. It has been reported that medial/lateral contact points deviate in the medial-lateral direction up to $\pm 2.6\text{mm}$ in artificial knee joints during walking [58]; therefore, we investigated the sensitivity of model predictions

across a similar range (± 4 mm). Tibiofemoral contact forces were directly proportional to the specified contact locations. A 2mm difference between model and subject contact-locations alters the predicted first peak of the medial contact force by 12% of body-weight and lateral contact force 10% of body-weight. We recommend that estimates of condylar contact based on center of pressure be used when this model is applied to biological knees.

Tibiofemoral alignment and contact locations primarily affected the medial-lateral load distribution by altering how the external loads and muscle forces passed relative to each compartment in the frontal-plane. In model conditions with subject-specific alignment, the knee joint moved medially causing the external knee adduction moment to decrease. Similarly, in model conditions with subject-specific contact locations, the contact locations shifted medially causing the external adduction moment relative to each compartment to decrease. In both cases, a reduced adduction moment from the external forces increased the lateral compartment contact force and decreased the medial compartment contact force. Altering the frontal-plane compartment contact locations also affected the frontal-plane muscle moment arms about each compartment. A medial shift in the contact location caused the muscle forces to increase their contribution to lateral compartment loading and decrease their contribution to medial compartment loading.

There are several limitations of this study. First, we were restricted to data from only a single individual because the design of our study necessitated a subject with an instrumented knee implant, post-operative non-neutral alignment, and radiographic images. Since we found directly proportional relationships between model-predictions and the geometric parameters, our results may apply across a range of individuals. Second, an assumption of our model was that tibiofemoral contact acted through single points in each compartment and the locations of these

points relative to the tibia reference frame remained stationary. The impact of this assumption is thought to be small since reports of the *in-vivo* frontal-plane medial/lateral contact locations from dual-orthogonal fluoroscopy and magnetic resonance images were not significantly different between 0° and 30° of weight-bearing knee flexion [63]. Third, we used a weighted static optimization approach to determine muscle weighting factors rather than an EMG driven approach. However, we found that the predicted medial-lateral distribution for each model and alignment condition were insensitive to variation of muscle weighting factors in static optimization. Since we applied the same objective function across all model conditions, our conclusions regarding the effect of the geometric parameters on model predictions are unlikely to depend on the method used to resolve muscle forces.

3.6 Conclusion

This study provides a novel articulating model of the knee to be used within a full-body musculoskeletal model with load bearing medial/lateral compartment joint structures for the prediction of these loads. For the participant in our study with genu valgum, specifying subject-specific lower-extremity alignment and medial/lateral compartment contact locations estimated from a standing anterior-posterior radiograph improved predictions of medial/lateral tibiofemoral contact forces. This suggests that frontal-plane alignment and frontal-plane medial/lateral compartment contact locations are important subject-specific model parameters that should be incorporated when predicting medial/lateral contact forces.

4. HOW PEDIATRIC OBESITY AFFECTS MUSCLE FUNCTION DURING WALKING³

4.1 Chapter Overview

The biomechanical mechanisms responsible for the altered gait in obese children are not well understood, particularly as they relate to increases in adipose tissue. The purpose of this study was to test the hypotheses that as body-fat percentage (BF%) increased: 1) knee flexion during stance would decrease while pelvic obliquity would increase; 2) peak muscle forces normalized to lean-weight would increase for gluteus medius, gastrocnemius, and soleus, but decrease for the vasti; and 3) the individual muscle contributions to center of mass (COM) acceleration in the direction of their primary function(s) would not change for gluteus medius, gastrocnemius, and soleus, but decrease for the vasti. We scaled a musculoskeletal model to the anthropometrics of each participant (n=14, 8-12 years old, BF%: 16-41%) and generated dynamic simulations of walking to predict muscle forces and their contributions to COM acceleration. BF% was correlated with average knee flexion angle during stance ($r=-0.54$, $p=0.024$) and pelvic obliquity range of motion ($r=0.78$, $p<0.001$), as well as with relative vasti ($r=-0.60$, $p=0.023$), gluteus medius ($r=0.65$, $p=0.012$) and soleus ($r=0.59$, $p=0.026$) force

³ The contents of this chapter have been published in:

Journal of Biomechanics (2014); 47(12): 2975-2982

Zachary F. Lerner
Sarah P Shultz
Wayne J. Board
Stacey Kung
Raymond C. Browning

production. Contributions to COM acceleration from the vasti were negatively correlated to BF% (vertical: $r=-0.75$, $p=0.002$, posterior: $r=-0.68$, $p=0.008$), but there were no correlation between BF% and COM accelerations produced by the gastrocnemius, soleus and gluteus medius. Therefore, we accept our first, partially accept our second, and accept our third hypotheses. The functional demands and relative force requirements of the hip abductors during walking in pediatric obesity may contribute to altered gait kinematics.

4.2 Introduction

Walking is the most common form of daily physical activity, yet obese children walk differently than nonobese children [64]. The altered gait exhibited by obese children have been associated with decreased gait stability [3] and reduced walking performance [65], as well as an increased prevalence of musculoskeletal pain [66] and pathology [67], which, collectively, may pose both short and long-term barriers to physical activity [68].

Gait analysis studies have shown that compared to nonobese children, obese children walk with wider step widths, increased medial-lateral motion, greater hip abduction, and reduced knee flexion during stance [3-5, 64]. Prior studies have also reported similar absolute knee extensor moments (Nm), greater absolute ankle plantarflexor moments (Nm), and greater normalized frontal plane moments ($\text{Nm}\cdot\text{kg}^{-1}\cdot\text{m}^{-1}$) of the hip/pelvis in obese vs. nonobese children [4, 5]. Therefore, compared to nonobese children, obese children may walk with reduced force requirements for the knee extensor muscles, but greater force requirements for both the plantarflexor and hip abductor muscles.

While it is well established that obese children walk differently than nonobese children, it is not clear why or how gait mechanics change as adiposity increases. Previous studies have used body mass index (BMI) to categorize participants into obese and nonobese groups. Since BMI

can be a poor predictor of pediatric adiposity [69], the altered gait strategy could be a consequence of either excess mass or a body composition that impairs locomotor ability. Furthermore, it is not yet known if the relationship between relative adiposity (i.e. body fat percentage, BF%) and gait mechanics is continuous in children or whether there is an adiposity threshold above which gait mechanics change, as has been proposed in obese adults [17].

Greater levels of adiposity appear to result in reduced muscle strength relative to total body mass [70-72] and gait mechanics appear to be sensitive to weakness of certain muscle groups [73]. Therefore, understanding the muscle force requirements of walking across a range of adiposity in children should provide insight into the possible imbalance between muscle and fat mass that may be responsible for the altered gait kinematics and kinetics. Additionally, certain muscles likely have functional requirements to accelerate and reposition the body during walking that are independent of adiposity and therefore may result in greater relative muscle force requirements with increasing BF% in children.

The purpose of this study was to investigate the relationship between adiposity and lower extremity kinematics, muscle force requirements, and individual muscle contributions to the acceleration of center of mass (COM) determined from musculoskeletal simulations of walking in children. We focused our investigation on the muscles implicated in the altered mechanics reported in previous studies [3, 4, 6, 71, 74] and which have primary roles acting to support (vasti (VAS), gastrocnemius (GAS), and soleus (SOL)), stabilize (gluteus medius (GMED)), and propel (GAS, and SOL) the whole body COM during the stance phase of walking [75, 76]. We hypothesized that as BF% increased: 1) knee flexion during stance would decrease while pelvic obliquity would increase; 2) peak muscle forces normalized to lean mass would increase for GMED, GAS, and SOL, but decrease for the VAS; and 3) the individual muscle contributions to

the acceleration of the COM in the direction of their primary function(s) would not change for GMED, GAS, and SOL, but decrease for the VAS.

4.3 Methods

Subjects

We used normalized frontal-plane hip joint moments between obese and non-obese children reported from prior literature [5] and power analysis to determine that a sample size of $n=14$ would allow us to detect strong [77], and meaningful correlation coefficients (e.g. $r=0.80$) with a power level of $\beta=0.95$ (SigmaPlot version 11.0, Systat Software, Inc., San Jose, CA). For this study, we defined a correlation coefficient as meaningful if greater than half of the variability in a gait measure could be attributed to adiposity. Gait analysis data from 14 children ages 8-12 years were selected from a larger study on the basis of creating a nearly continuous and even distribution of BF% from lean to obese (BF% 16-41%) (Table 4.1). We also analyzed subsets of 5 non-obese (BF% < 25%) and 5 obese children (BF% > 35%) children to allow comparisons between our results and previously published data. Participants were selected who did not report lower-extremity malalignment and were relatively tall, so as to minimize musculoskeletal model scaling (see below). Exclusion criteria included any neuromuscular, musculoskeletal, or cardiovascular disorder, other than obesity, impacting safe participation in the study. Prior to data collection, the study was approved by the Massey University Human Ethics Committee and informed written assent and consent was obtained from the participants and their parents, respectively.

Table 4.1 Subject characteristics and analyzed walking speed (values are mean (SD)). * denotes a significant difference between the obese and nonobese group.

	N	Age (years)	Height (cm)	Mass (kg)	Lean Mass (kg)	BF%	LEF%	Walking Speed (m•s)	Dim. less Speed	Gender (# Male)
All	14	10.1 (1.5)	151 (10.8)	54.9 (22.5)	36.3 (11.6)	29.6 (8.7)	45.2 (3.3)	0.96 (0.08)	0.34 (0.02)	6
Obese	5	10.6 (1.1)	157 (8.0)	77.3 (7.9)	46.7 (12.1)	37.6 (4.0)	45.2 (2.7)	0.98 (0.08)	0.34 (0.02)	2
Overweight	4	10.5 (1.9)	151 (8.5)	50.8 (8.3)	33.6 (6.1)	32.2 (3.1)	45.6 (2.3)	0.93 (0.1)	0.33 (0.03)	0
Nonobese	5	9.4 (1.6)	145 (13.5)	35.9 (21.1)	28.1 (6.2)	19.4 (2.2)	44.8 (4.9)	0.98 (0.08)	0.35 (0.02)	4

Experimental Protocol

We quantified body composition, specifically BF% and lean tissue mass, for each subject using dual x-ray absorptiometry (DEXA, Hologic Discover, Bedford, MA). Participants walked barefoot on an instrumented treadmill at self-selected speeds. Self-selected speed was identified as the average walking speed of 5 overground trials [78]. Participants had similar self-selected walking speeds and dynamically similar dimensionless walking speeds [79] (Table 4.1). Participants were given a familiarization period on the treadmill that lasted several minutes and was terminated upon verbal and visual confirmation of comfortable gait.

Experimental Data

Three-dimensional kinematic data were collected using a 9-camera motion capture system (VICON MX System, Vicon, Oxford, UK) collecting at 200 Hz, while kinetic data were collected using a dual-belt, force measuring treadmill (Fully Instrumented Treadmill; Bertec Corp, Columbus, OH) collecting at 1000 Hz. Marker trajectory and ground reaction force data were digitally low-pass filtered at 5 Hz and 12 Hz, respectively, using fourth-order zero-lag Butterworth filters. We used an extensive, obesity-specific marker set methodology, reported in detail previously that was specifically developed to reduce the effects of subcutaneous adiposity

obscuring the motion of the underlying skeleton, particularly around the pelvis [7]. Briefly, the methodology is as follows: Reflective markers placed over the 7th cervical vertebrae, acromion processes, right scapular inferior angle, sterno-clavicular notch, xyphoid process, 10th thoracic vertebrae, posterior-superior iliac spines, medial and lateral epicondyles of the femurs, medial and lateral malleoli, calcanei, first metatarsal heads, second metatarsal heads, and proximal and distal heads of the 5th metatarsals. A digitizing pointer (C-Motion, Germantown, MD) was used to mark the anterior superior iliac spines (ASIS) and iliac crests, while marker clusters (four non-collinear markers affixed to a rigid plate) were adhered to the thighs, shanks, and sacrum.

Musculoskeletal Modeling

To predict muscle forces, we used OpenSim [10] to generate dynamic musculoskeletal simulations from the experimental gait data of two representative strides for each participant. Anatomical landmarks were used to scale a generic, 12 segment musculoskeletal model with 23 degrees of freedom (DOF) and 92 muscle-tendon actuators [12, 31] to the individual anthropometrics (i.e. total body mass and segment length) of each participant. Model DOF included a ball-and-socket joint at the third lumbar vertebra, 3 translations and 3 rotations at the pelvis, a ball-and-socket joint at each hip, single DOF tibiofemoral joints with anterior/posterior and superior/inferior translations prescribed as a function of knee flexion [30, 31], and revolute ankle and subtalar joints.

Inertial properties of each segment were scaled as a function of segment length and total body mass, regardless of BF%. Lower extremity joint angles were calculated using OpenSim's inverse kinematics analysis, which minimized the errors between markers on the scaled model and experimental marker trajectories. Segment masses of the pelvis, thigh and shank were

adjusted during a residual reduction algorithm that minimizes the residual forces and moments acting on the model arising from dynamic inconsistency [10].

We resolved individual muscle forces from net joint moments using a weighted static optimization approach implemented in a custom OpenSim plugin [12, 29]. The objective function minimized the sum of squared muscle activations, while incorporating individual muscle weighting constants (3 for the hamstrings, 7 for the gastrocnemius, and 1 for all remaining muscles) that were previously determined by minimizing the difference between model estimated tibiofemoral forces and those measured experimentally from an instrumented knee joint replacement [12, 32]. The muscle forces predicted using static optimization are not sensitive to maximum isometric force when the maximum isometric force of all of the muscles are scaled uniformly and the muscles operate below maximal activation. Therefore, because we lacked the information to scale the maximum isometric force of individual muscles (see limitations), the maximum isometric forces were scaled uniformly only if muscles reached maximal activation.

Individual muscle contributions to the acceleration of the center of mass for each simulated gait cycle were quantified using an induced acceleration analysis method described previously by Lin et al., implemented in a validated OpenSim plugin [76, 80]. This method was selected because it allowed us to use the muscle forces predicted from static optimization. While described previously in extensive detail, this methodology resolves individual muscle contributions to the acceleration of the COM by solving the equations of motion which describe the dynamics of the simulation while each muscle is applied independently [76]. This approach assumes that the interaction between the feet and the treadmill occurs at 5 contact points

geometrically located around the foot. Contact conditions (i.e. constraint type) for each point are modulated based on the phase of the gait cycle determined from the ground reaction forces.

To ensure our simulations were dynamically and physiologically representative, we analyzed the resulting residual forces and muscle activations, respectively. The average residual force applied to the COM of the musculoskeletal model in each coordinate direction, for all participants, was less than 3% body-weight, suggesting that our musculoskeletal simulations and experimental data were reasonably dynamically consistent. Average residuals, as a percentage of body weight, did not increase with BF%. Additionally, we found that the on/off timing of the muscle activations were in close agreement with experimentally measured EMG reported previously for the literature for the GAS [78], GMED [81], VAS [78], and SOL [82].

In addition to normalizing muscle forces to body-weight, we also normalized the muscle forces to lean-weight as an estimate for the force requirement relative to the size/strength of the tissue responsible for producing force, skeletal muscle fibers. This was done to determine which muscles might be most susceptible to mechanical overload/fatigue with increasing BF%. We present the joint angles, peak muscle forces (absolute, body-weight normalized, and lean-weight normalized), and individual muscle contributions to the acceleration of the COM from the right leg, normalized to each gait cycle, averaged across two representative gait cycles for each subject.

Statistical Analysis

We used Pearson product-moment correlation analysis to determine the association between BF% and our outcome measures. Student's t-tests were used to determine if there were significant differences in kinematic and kinetic variables between the obese/nonobese subsets.

SigmaPlot, version 11.0 (Systat Software, Inc., San Jose, CA) was used to perform the statistical analyses, where $p < 0.05$ defined significance.

4.4 Results

There was a moderate negative correlation between average and peak early stance knee angle and BF% and a strong positive correlation between pelvic obliquity and BF% (Figure 4.1). The obese subset had a significantly greater pelvic obliquity range of motion (12.4° vs. 8.1° , $p < 0.001$), and significantly reduced average early stance knee flexion angle (8.8° vs. 12.0° , $p = 0.024$) compared to the nonobese subset (Figure 4.1).

Absolute GAS, SOL and GMED muscle forces (N) had moderate-strong positive correlations to BF% (Figure 4.2, Table 4.2). Body-weight normalized VAS and SOL forces had strong and moderate negative correlations to BF%, respectively. The correlation between BF% and lean-weight normalized forces were positive and moderate-strong for GMED and SOL, while negative and moderate-strong for the VAS. Compared to the nonobese subset, the obese subset had significantly greater absolute muscle forces, except for VAS (Figure 4.2). Body-weight normalized forces were lower for both the SOL and VAS between the obese vs. nonobese children. Lean-weight normalized GMED and SOL forces were 43% (1.80 vs. 1.26 lean-body-weights ($p = 0.011$)) and 17% (4.61 vs. 3.94 lean-body-weights ($p = 0.010$)) greater, respectively, while lean-weight normalized VAS forces were 36% (0.64 vs. 1.0 lean-body-weights ($p < 0.008$)) lower in the obese vs. nonobese subsets.

There were moderate-strong negative relationships between BF% and both the superior and posterior accelerations of the COM induced by the VAS (Figure 4.3, Table 4.3). We found no other significant relationships between BF% and the contributions to the acceleration of the COM for the other muscles analyzed. Contributions to the superior and posterior accelerations of

the COM induced by the VAS were 108% (0.51 m/s^2 vs. 1.70 m/s^2 ($p < 0.001$)) and 81% (0.35 m/s^2 vs. 0.81 m/s^2 ($p < 0.001$)) lower, respectively, in the obese vs. the nonobese subsets.

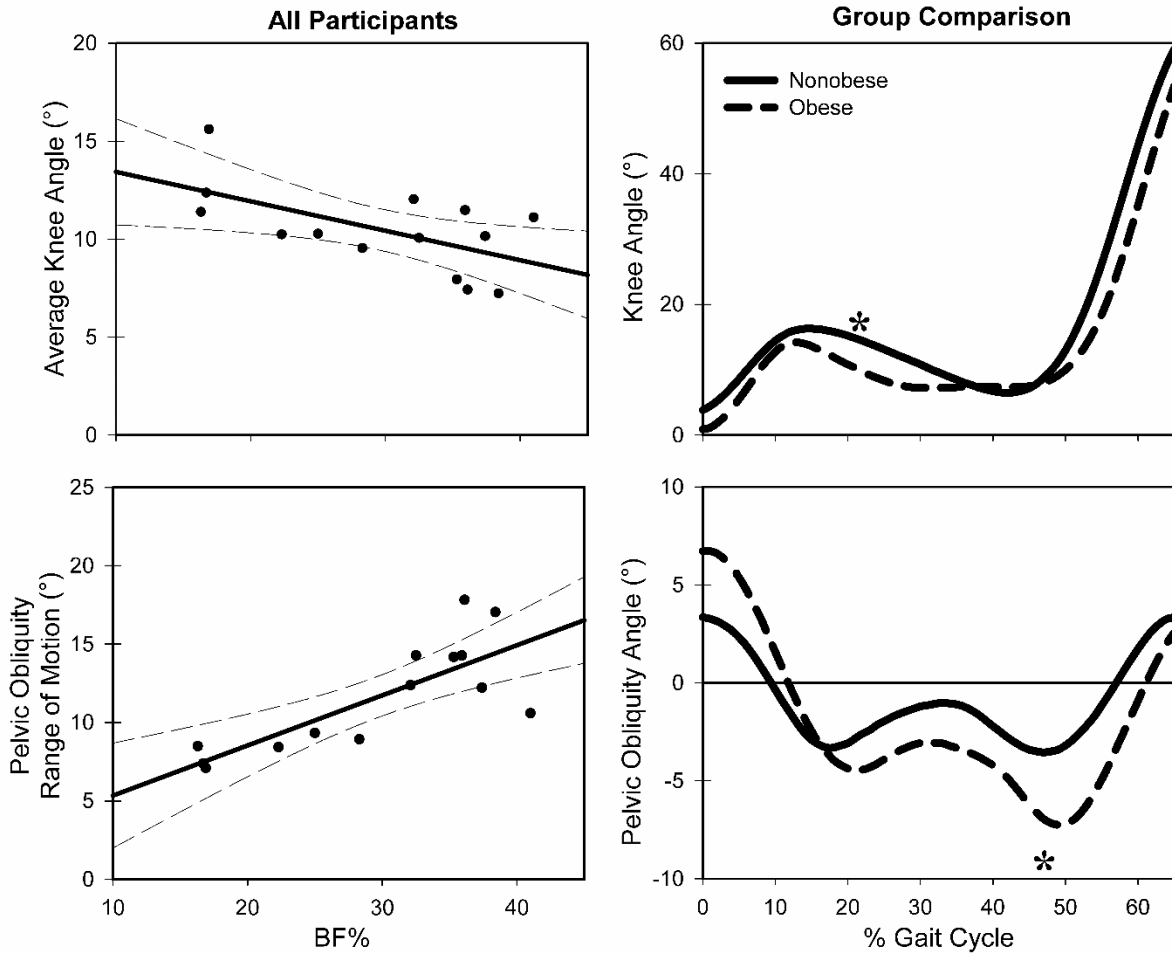


Figure 4.1 *Left Panels*: The relationship between BF% and average knee angle during stance (top) and range of pelvic obliquity (bottom). The bold regression lines represent significant relationships. The dashed lines represent the 95% confidence intervals. The regression equations describing the relationships between BF% and average knee flexion angle during stance (θ_{Knee}), and pelvic obliquity (θ_{PO}) were found to be $\theta_{\text{Knee}} = -0.15 \cdot \text{BF\%} + 14.9$ and $\theta_{\text{PO}} = 0.32 \cdot \text{BF\%} + 2.3$, respectively. *Right Panels*: Mean early-mid stance knee joint angles (top) and pelvic obliquity (bottom) for the obese (dashed) and nonobese (solid) subsets during walking. Compared to the nonobese subset, the obese subset exhibited a more extended knee during stance and greater range of pelvic obliquity. *Denotes a significant difference.

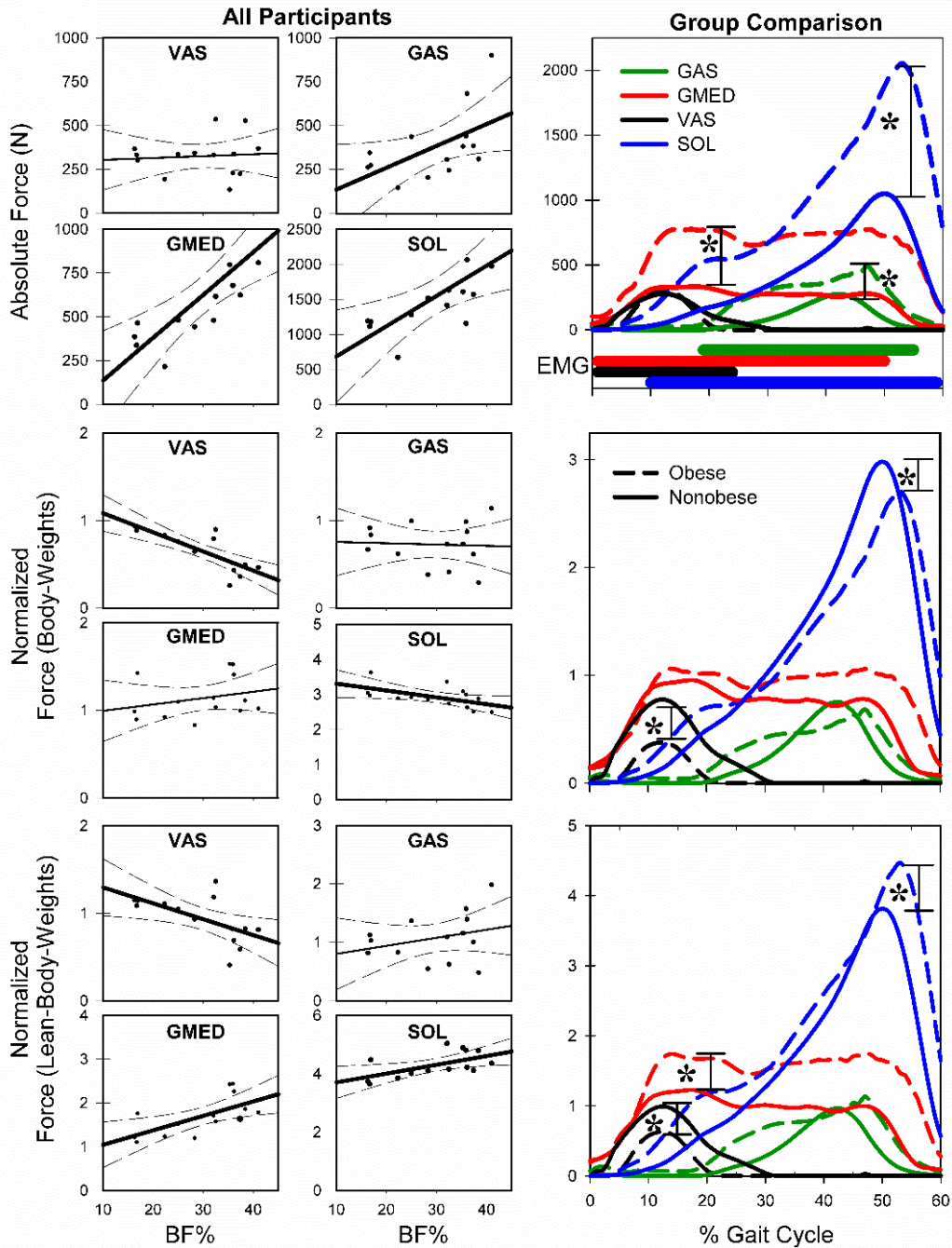


Figure 4.2 *Left Panels:* The relationship between BF% and absolute (top 4), body-weight normalized (middle 4), and lean-weight normalized (bottom 4) VAS, GMED, GAS, and SOL muscle forces. The bold regression lines represent significant relationships. The dashed lines represent the 95% confidence intervals. The regression equations describing the significant relationships between BF% and absolute (F_{AB}), BW normalized (F_{BW}), and, LW normalized (F_{LW}) muscle forces were $F_{GMED, AB} = 24.4 \cdot BF\% - 108$, $F_{GAS, AB} = 12.5 \cdot BF\% - 9.6$, $F_{SOL, AB} = 44.3 \cdot BF\% + 230$, $F_{SOL, BW} = -0.020 \cdot BF\% + 3.5$, $F_{VAS, BW} = -0.022 \cdot BF\% + 1.3$, $F_{GMED, LW} = 0.033 \cdot BF\% + 0.72$, $F_{SOL, LW} = 0.030 \cdot BF\% + 3.4$, and $F_{VAS, LW} = -0.018 \cdot BF\% + 1.5$. *Right Panels:* Mean absolute (top), BW normalized (middle), and LW normalized (bottom) muscle forces for the obese (dashed) and nonobese (solid) subsets. The EMG on/off timing taken from the literature for the GAS [78], GMED [81], VAS [78], and SOL [82] is presented below the abscissa of the top plot (A). *Denotes a significant difference.

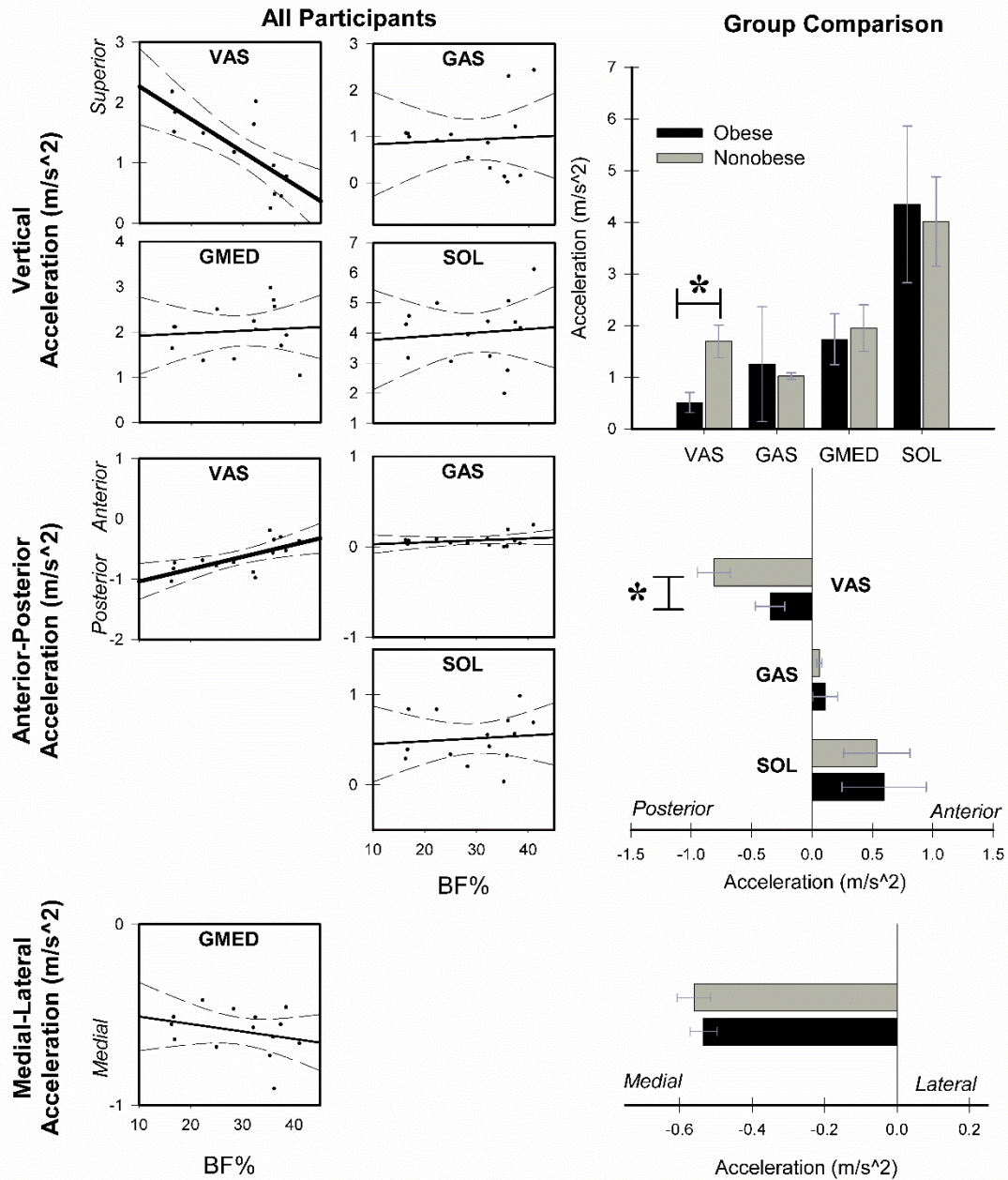


Figure 4.3 *Left Panels*: The relationship between BF% and the individual muscle contributions to the acceleration of COM, averaged over the gait cycle, in the superior (top), anterior-posterior (middle), and medial-lateral (bottom) directions. The bold regression lines represent significant relationships. The dashed lines represent the 95% confidence intervals. The regression equations describing the significant relationships between BF% and induced acceleration to the COM in the superior (IAA_S) and posterior directions (IAA_P) were $IAA_{S,VAS} = -0.054 \cdot BF\% + 2.81$ and $IAA_{P,VAS} = -0.21 \cdot BF\% - 1.24$, respectively. *Right Panels*: Individual muscle contributions to the acceleration of the COM in the superior-inferior (top), anterior-posterior (middle), and medial-lateral (bottom) directions for the obese (black) and nonobese (gray) subsets.

Table 4.2 The relationship between BF% and absolute, body-weight (BW) normalized, and lean-weight (LW) normalized peak muscle forces reported as Pearson product-moment correlation coefficients. Bold denotes a significant correlation or difference between the obese and non-obese groups.

Muscle	Absolute Force		BW Normalized Force		LW Normalized Force	
	r	p	r	p	r	p
VAS	0.08	(p=0.770)	-0.82	(p<0.001)	-0.60	(p=0.023)
GMED	0.76	(p=0.001)	0.27	(p=0.357)	0.65	(p=0.012)
GAS	0.55	(p=0.044)	0.05	(p=0.861)	0.29	(p=0.319)
SOL	0.66	(p=0.040)	-0.55	(p=0.015)	0.59	(p=0.026)

Table 4.3 The relationship between BF% and the average individual muscle contributions to the acceleration of the COM for select muscles reported as Pearson product-moment correlation coefficients (r) and the average individual muscle contributions to the acceleration of the COM for select muscles between the obese and nonobese subsets. Bold denotes a significant correlation or difference between the obese and non-obese groups.

Direction	Muscle	Correlation to BF% (r)	p	Obese (m•s ⁻²)	Nonobese (m•s ⁻²)	p
Superior	VAS	-0.75	(p=0.002)	0.51	1.70	(p<0.001)
	GMED	0.09	(p=0.768)	1.73	1.95	(p=0.489)
	GAS	0.06	(p=0.833)	1.25	1.02	(p=0.651)
	SOL	<0.01	(p=0.995)	4.3	4.01	(p=0.920)
Anterior	GAS	0.27	(p=0.343)	0.11	0.06	(p=0.340)
	SOL	0.10	(p=0.732)	0.60	0.54	(p=0.772)
Posterior	VAS	-0.68	(p=0.008)	-0.35	-0.81	(p<0.001)
Medial	GMED	0.23	(p=0.335)	0.61	0.56	(p=0.665)

4.5 Discussion

We sought to investigate the effects of adipose tissue on the sagittal plane knee angle, frontal plane pelvic angle, relative muscle forces, and muscle contributions to COM acceleration during walking in children. There was a significant negative correlation between BF% and the average knee flexion angle during stance, and a significant positive correlation between BF% and pelvic obliquity range of motion; thus, we accept our first hypothesis. GMED and SOL had significant positive correlations to BF% but GAS did not; thus we partially accept our second hypothesis. We accept our third hypothesis, as the individual contributions to the acceleration of the COM were similar for all muscles, but reduced for VAS in the vertical and anterior-posterior directions. A post hoc-analysis revealed generally similar, but weaker relationships between BMI

and outcome measures vs. the relationships determined with BF%. Therefore, while BF% appears to be a more accurate predictor of gait measures, BMI could be used to predict gait changes in obese children.

The changes in muscle forces between the obese and non-obese subsets were consistent with what would be expected from the joint moments reported in the literature. Our finding of similar absolute VAS forces between our obese and nonobese subjects are consistent with previous reports of similar absolute knee extensor moments [4] between obese and non-obese children. Greater absolute GAS and SOL forces, and lower body-weight normalized SOL forces in obese participants corroborates reports of greater ankle plantar flexor moments in obese children [4]. Finally, larger absolute GMED forces are consistent with reports of greater absolute hip abductor moments in obese children, compared to non-obese children [6].

The predictions of GAS, GMED, VAS, and SOL muscle forces and their contributions to the superior-inferior and anterior-posterior acceleration of the COM found in our non-obese subsets are similar, with some small differences, to those previously reported at similar walking speeds for normal weight children [83, 84]. In particular, compared to these previous reports, we found lower GAS forces and induced acceleration contributions, which is likely due to our use of weighting factors in the static optimization objective function.

We found that lean-weight normalized GMED force had a strong positive correlation to BF%. This suggests that as BF% increases, GMED may operate closer to its maximum force production and therefore be susceptible to functional weakness/fatigue during walking. In addition to supporting the torso in the frontal plane during single limb stance, GMED repositions the COM from one stance leg to the other during double support [85]. While the contribution of GMED to the medial acceleration of the COM did not change with BF%, there was a strong

positive relationship between pelvic obliquity range of motion, which is controlled primarily by GMED, and BF%. This may suggest that the locomotor control strategy for muscle function prioritizes the fulfillment of functional roles (i.e. supporting, braking/propelling, and balancing the body) over maintaining normal joint angles.

Greater pelvic obliquity during single limb stance results in a drop of the contralateral hip joint center. In order to maintain toe clearance of the swing limb, either the stance limb would need to become more extended or the swing limb to become more flexed (Figure 4.4). Walking with a straighter leg is likely more economical than the alternative and would allow normal swing limb kinematics, which appear to be tightly controlled [86]. The strong negative correlation between pelvic obliquity range of motion and average knee flexion angle during stance corroborate this theory (Figure 4.5). Since walking with a straighter leg results in reduced knee extensor moments, this may explain the reduction in body-weight and lean-weight normalized VAS force requirements in children with greater BF%. The reduced knee extensor muscle strength reported in obese children [70] may be a result of, rather than the cause of, walking with a straighter limb during stance.

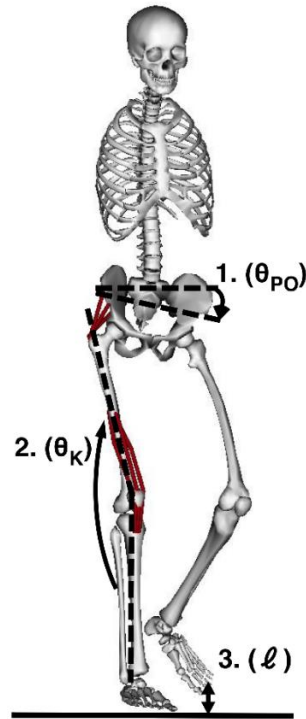


Figure 4.4 The potential relationship between increased pelvic obliquity, stance limb knee flexion, and toe clearance during single support during walking. (1) Increased pelvic obliquity results in a drop of the contralateral hip joint center, while (2) the stance limb becomes more extended to allow the swing limb (3) to maintain toe clearance.

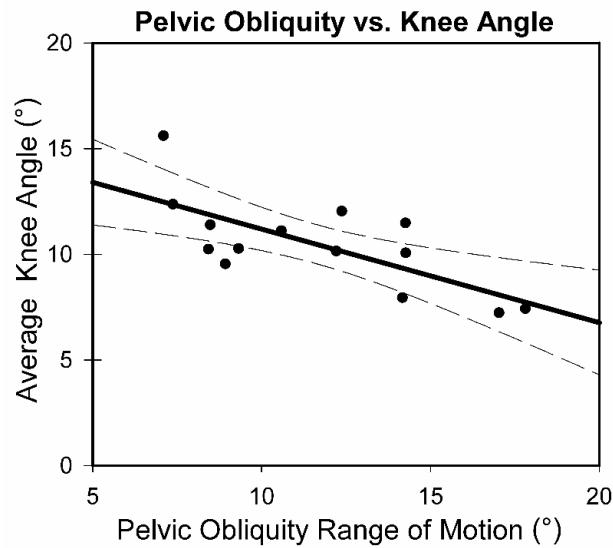


Figure 4.5 The potential relationship between increased pelvic obliquity, stance limb knee flexion, and toe clearance during single support during walking. (1) Increased pelvic obliquity results in a drop of the contralateral hip joint center, while (2) the stance limb becomes more extended to allow the swing limb (3) to maintain toe clearance.

The negative correlations between the VAS contributions to both the superior and posterior COM accelerations and BF% is consistent with our finding of reduced VAS forces with increasing BF%. It is likely that a greater proportion of the COM acceleration in the vertical direction is attributed to a more aligned skeleton. Apart from the VAS, the other analyzed muscles had contributions to COM acceleration that were not correlated to BF% and not significantly different between the obese and non-obese subsets. This indicates that the ankle plantarflexors (GAS and SOL) and hip abductors (GMED) have functions to reposition the body that are independent of BF%.

It has been suggested that walking with a straighter leg may be a compensatory mechanism to reduce the knee extensor moment during early stance [4]. Conversely, it has been reported that maintaining normal gait kinematics is insensitive to weakness of the VAS, the muscles responsible for producing this moment during early-mid stance [73]. Furthermore, the vastus lateralis and vastus medialis muscles operate at less than 30% and 15% of maximum voluntary isometric contraction (MVIC), respectively, during the stance phase of walking [87], indicating that these muscles are minimally active during normal gait. The strong negative correlation between lean-weight normalized VAS forces and BF% indicates that the VAS remains relatively unburdened by increased adiposity. Together with the previous literature, these findings would suggest that additional adiposity in obesity would not likely lead to unsustainable VAS force requirements during walking. Alternatively, normal gait mechanics appears to be very sensitive to GMED weakness [73]. Furthermore, GMED operates at ~70% of MVIC during walking in normal weight individuals [81]. These findings indicate that GMED is not only highly active during gait but also has a large potential to influence gait kinematics if overloaded. Our results support these previous findings and indicate that as BF% increases

GMED is unable to sustain/maintain normal pelvic region kinematics while fulfilling functional requirements to reposition the COM. Children with high BF% are not able to walk in such a way that reduces the relative requirements of GMED because the frontal plane lacks a redundant biomechanical mechanism to support the body during single limb stance.

It was initially surprising to find that, unlike the SOL, lean-weight normalized GAS forces were not significantly positively correlated with BF%. We expected both muscles to have positive relationships between their lean-weight normalized force outputs and BF% due to the increasing imbalance between fat and muscle mass as BF% increases. However, there was greater variability in the peak GAS forces, which limited the significance of the positive correlation.

The results of this study have important clinical implications. Hip abductor weakness/fatigue in overweight and obese children may hinder postural control [88] and thus prevent these children from being able to safely engage in sustainable weight bearing physical activity. In addition, increased frontal plane motion of the pelvis alters hip joint mechanics and articulation of the femoral head with the acetabulum, which has been implicated in slipped capital femoral epiphysis [66]. Walking with greater frontal plane rotation of the pelvis can also strain the low back and likely contribute to increased prevalence of low back pain in pediatric obesity [89]. Importantly, obese children and adults appear to exhibit similar gait mechanics [90]. This suggests that without intervention in children with high BF%, the altered relative muscle force requirements, associated gait modifications, and implicated musculoskeletal pain/pathologies will persist and obstruct physical activity participation throughout life.

A limitation of this study was that the sample size was relatively small. Model limitations included scaling a generic model to the anthropometrics of each participant, a knee joint with no

frontal plane degree of freedom, and muscle parameters based on adult physiology. We sought to limit the impact of these limitations by 1) selecting taller participants to minimize the amount of model scaling required in order to reduce the potential negative influence on muscle moment arms, and 2) excluding participants with significant knee joint malalignment to minimize the impact of the single DOF knee joint on lower-extremity kinetics. The literature suggests that intrinsic muscle contractile properties [91] and muscle strength/fatigue *relative* to fat-free mass for certain muscle groups (e.g. knee extensors) [92] are not affected by pediatric obesity. We found that muscle force predictions were not affected by the strength of the model when maximum isometric forces were scaled uniformly so long as muscles operated below full activation. This suggests that model limitations/assumptions would affect obese/non-obese children equally; therefore, we are confident that the relative differences in simulation outcomes between participants are a result of the experimental data and not model limitations. Another limitation was that we did not collect EMG data to compare to the results of our musculoskeletal simulations, but while this comparison would have been desirable, our simulations were not EMG driven and did not require them. Additionally, this musculoskeletal model and optimization method have been used to predict muscle activations in close agreement with experimental EMG in children [12], and a qualitative comparison between the results of this study and published EMG (Figure 4.2) demonstrated close agreement. Lastly, excess adiposity may obscure the motion of the underlying skeleton. These inaccuracies were minimized as much as possible by implementing an obesity-specific marker set methodology.

4.6 Conclusion

In conclusion, as BF% increased, we found reduced early stance knee flexion angles, increased pelvic obliquity range of motion, decreased relative demand of the VAS, but increased

relative demand of GMED and SOL. This suggests that changes in the relative force requirements of lower extremity muscles during walking may lead to the altered walking mechanics exhibited in children as BF% increases. Activities and interventions should facilitate hip abductor and plantar flexor strengthening, to normalize gait in the long-term, while reducing fatigue to these essential and at risk muscles in the short-term. Future studies should investigate the effects of altered gait mechanics on the osteoarticular loading environment in children with a range of adiposities to further elucidate the underlying mechanisms responsible for the negative effects of pediatric obesity on the musculoskeletal system.

5. HOW PEDIATRIC OBESITY AFFECTS MEDIAL AND LATERAL TIBIOFEMORAL CONTACT FORCES DURING WALKING⁴

5.1 Chapter Overview

With the high prevalence of pediatric obesity there is a critical need for structured physical activity during childhood. However, altered tibiofemoral loading during physical activity in obese children likely contribute to their increased risk of orthopedic disorders of the knee. The goal of this study was to determine the effects of pediatric obesity and walking duration on medial and lateral tibiofemoral contact forces. We collected experimental biomechanics data during treadmill walking at $1 \text{ m}\cdot\text{s}^{-1}$ for 20 minutes in 10 obese and 10 healthy-weight 8-12 year-olds. We created subject-specific musculoskeletal models using radiographic measures of tibiofemoral alignment and centers-of-pressure, and predicted medial and lateral tibiofemoral contact forces at the beginning and end of each trial. Obesity and walking duration affected tibiofemoral loading. At the beginning time-point (1st minute after a 5 minute acclimation period), the medial load share (percent of the total axial load passing through the medial compartment) during stance was 85% in the obese children vs. 63% in the healthy-weight children. At the end time-point (20th minute), the medial load share was 90% in the obese

⁴ The contents of this chapter are under review in:

Medicine and Science in Sports and Exercise (Under Review)

Zachary F. Lerner
Wayne J. Board
Raymond C. Browning

children vs. 72% in the healthy-weight children. Medial compartment loading rates were 1.78 times greater in the obese vs. the healthy-weight participants. The medial compartment loading rate increased 17% in both groups at the end vs. the beginning time-point ($p=0.001$). We found a strong linear relationship between body-fat percentage and the medial-lateral load distribution ($r^2=0.79$). Altered tibiofemoral loading during walking in obese children may contribute to their increased risk of knee pain and pathology. Longer walking durations may increase these risks.

5.2 Introduction

Pediatric obesity is a worldwide health concern with cardiovascular and orthopedic consequences for the child and future adult. Obese children have an increased risk of developing orthopedic disorders of the knee [1]. Dynamic mechanical loads incurred during physical activity (e.g. walking), affect the development and maintenance of joint tissues and surrounding bone [93, 94]. Compared to healthy-weight children, obese children walk with larger frontal [4, 6] and sagittal [6] plane knee moments, suggesting obese children have greater tibiofemoral contact forces that are more medially distributed. It has been theorized that the combination of larger magnitudes and altered application of joint loads in obese children may lead to bone and joint alterations [67], such as growth-plate suppression, that result in knee malalignment [95]. However, no studies have quantified medial and lateral tibiofemoral joint contact forces in obese children. Therefore, it is unknown how pediatric obesity affects the distribution, magnitudes, and loading rates of tibiofemoral contact forces during walking.

From a cardiovascular and caloric-balance standpoint, obese children can benefit by participating sufficient daily physical activity. Children are recommended to engage in at least 60 minutes of moderate to vigorous physical activity each day [96], and clinicians recommend physical activity bout durations of at least 10 minutes to improve cardiovascular capacity [97].

During walking, obese children have greater relative force requirements for several muscles, including the hip abductors, which function to control the kinematics and kinetics of the whole body center of mass in the frontal plane [9]. Therefore, these muscles may fatigue in obese children during extended periods of walking, which may affect the medial-lateral distribution of tibiofemoral contact forces by altering the dynamics of the body in the frontal plane. Our incomplete understanding of how childhood obesity affects joint loading during continuous bouts of activity limits our ability to evaluate the long-term risk-benefit ratio of prescribed physical activity on the musculoskeletal system.

To improve orthopedic treatment and determine safe physical activity guidelines for obese children, clinicians need to understand how obesity and activity duration affects the knee joint loading environment during weight-bearing activities like walking. Knowledge of the magnitudes and medial-lateral distribution of knee loads in obese children may elucidate our understanding of the development of orthopedic disorders affecting the knee. Recent advancements in motion capture techniques for use with obese individuals [7] and musculoskeletal models capable of incorporating subject-specific parameters and resolving medial and lateral tibiofemoral compartment forces [8] make such an investigation possible.

The purpose of this study was to determine how obesity and walking duration affect the knee joint loading environment in children. We hypothesized that 1) obese children would have larger tibiofemoral contact forces that were more medially distributed than healthy-weight children, and 2) walking duration would result in greater medial load share in all children, but that there would be greater changes in the obese children. To evaluate our hypotheses, we collected experimental biomechanics data during treadmill walking for 20 minutes in obese and healthy-weight children, quantified each participant's anthropometrics and skeletal structure

using radiography, created subject-specific musculoskeletal models, and estimated the contact forces in the medial and lateral compartments of the knee.

5.3 Methods

Participants

This study was approved by Colorado State University’s Human Research Institutional Review board, and informed written assent and consent was obtained from the participants and their parents, respectively. This was a cross-sectional study of a convenience sample. Ten (10) obese (4 female) children with a BMI-Z score greater than the 95th percentile and 10 healthy-weight (5 female) children with a BMI-Z score between the 5th and 85th percentiles participated in our study. Subject characteristics and anthropometrics are presented in Table 5.1. Exclusion criteria included any disorder, other than obesity, of the neuromuscular, musculoskeletal, or cardiovascular systems that would preclude safe participation in the study.

Table 5.1 Participant characteristics. Values are mean (SD). Bold denotes a significant difference between groups.

	Obese	Healthy-Weight
Body Mass (kg)	57.5 (11.7)	31.7 (6.6)
Leg Length (m)	0.72 (0.05)	0.68 (0.06)
Body Fat (%)	42.1 (5.0)	26.4 (3.0)
BMI-Z (Percentile)	98 (2)	34 (23)
Age (years)	9.5 (0.9)	9.6 (1.4)

Body composition for each participant was quantified using dual x-ray absorptiometry (DXA) (Whole-Body Scan, Hologic Discover, Bedford, MA). The placement and orientation of each participant’s lower-extremity and feet on the imaging table were standardized using a custom jig. We also captured a higher-resolution DXA scan (1mm Line Spacing, <1mm Point Resolution) of each participant’s right knee. To investigate the periarticular skeletal structure in the medial and lateral tibial epiphyses, we defined a medial and lateral regions of interest (ROI)

on the knee DXA scan and measured the areal bone mineral density (BMD) similar to the method used by Lo et al. [98] (Figure 5.1).

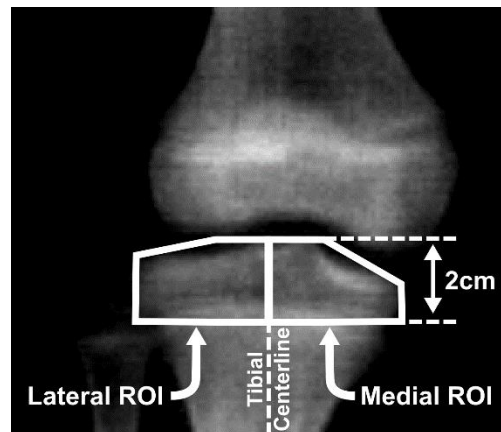


Figure 5.1 Anteroposterior high resolution DXA radiograph of a participant's right knee. The white rectangle rectangles are the ROIs used to measure medial and lateral tibial epiphyses BMD.

Experimental Walking Protocol

Participants walked on an instrumented treadmill (Bertec Corp, Columbus, OH) at $1.0 \text{ m}\cdot\text{s}^{-1}$ for 20 minutes. We collected kinematic data using a ten-camera, three-dimensional motion capture system (Nexus, Vicon, Centennial, CO). We used a custom marker set and calibration procedure designed to account for adiposity and improve tracking of the underlying skeleton [7]. While reported in extensive detail previously, this approach, in short, is as follows: reflective markers were placed over the 7th cervical vertebrae, acromion processes, right scapular inferior angle, sterno-clavicular notch, xyphoid process, 10th thoracic vertebrae, posterior-superior iliac spines, medial and lateral epicondyles of the femurs, medial and lateral malleoli, calcanei, first metatarsal heads, second metatarsal heads, and proximal and distal heads of the 5th metatarsals. We used a digitizing pointer (C-Motion, Germantown, MD) to probe through overlying soft-tissue and mark the anterior superior iliac spines (ASIS) and iliac crests on their bony locations. Marker clusters (four non-collinear markers affixed to a rigid plate) were adhered to the thighs,

shanks, and sacrum. To account for adiposity surrounding the pelvis, post-processing (Visual 3D, C-Motion, Germantown, MA) was used to define the digital ASIS and iliac crest landmarks relative to the sacral cluster and generate virtual markers for subsequent segment tracking. Ground reaction force data were recorded at 1000Hz and low-pass filtered at 12 Hz using a fourth order zero-lag Butterworth filter. Kinematic data were recorded at 100Hz and low-pass filtered at 5 Hz using a fourth order zero-lag Butterworth filter.

We also recorded electromyography (EMG) data (Noraxon, Scottsdale, AZ) from the medial gastrocnemius, vastus lateralis, vastus medialis, biceps femoris long-head, and semimembranosus muscles using standard procedures [28]. EMG data were recorded at 1,000 Hz, band-pass filtered at 16–380 Hz, full-wave rectified, and low-pass filtered at 7Hz to generate a linear envelope.

Musculoskeletal Model Description

We introduced a knee mechanism into a full-body OpenSim gait model that was capable of incorporating subject-specific knee parameters (tibiofemoral alignment and centers-of-pressure) and resolving medial and lateral compartment contact forces. We conducted a model validation and sensitivity analysis in a prior study [8]. The full-body model had 18 body segments and 92 muscle-tendon actuators [31, 99], and has been used in studies investigating muscle function and joint loading in children [9, 12]. The knee mechanism included joint structures to represent the medial and lateral tibiofemoral compartments. These structures articulated over the surface of the femoral condyles during knee flexion-extension and bore the medial and lateral contact forces required to balance the net reaction forces and frontal-plane moments across the tibiofemoral joint. In our prior validation study we used experimental walking data from an individual with an instrumented knee implant and compared model

predictions to the *in-vivo* measurements. Predictions were sensitive to tibiofemoral alignment and centers-of-pressure. When these parameters were specified via anterior-posterior radiograph, the model accurately predicted medial and lateral contact forces (14).

Subject-Specific Model Building

We scaled our model for each subject using markers placed on anatomical landmarks of each segment (Figure 5.2A). In this way, segment inertial properties, joint articulations, muscle moment arms, muscle attachments, and muscle length properties (muscle-tendon, tendon slack, and optimal fiber lengths) were scaled to each individual's anthropometrics. Next, we modified each participant's scaled model and created a subject-specific model by specifying their lower-extremity alignment, medial and lateral tibiofemoral centers-of-pressure, and segment masses determined from the DXA radiographs (Figure 5.2B-D, detailed below). We also ensured that the distances between the knee joint center and the medial and lateral femoral epicondyle markers in each subject-specific model were within a $\frac{1}{2}$ cm to the actual, physical distances measured on each knee radiograph.

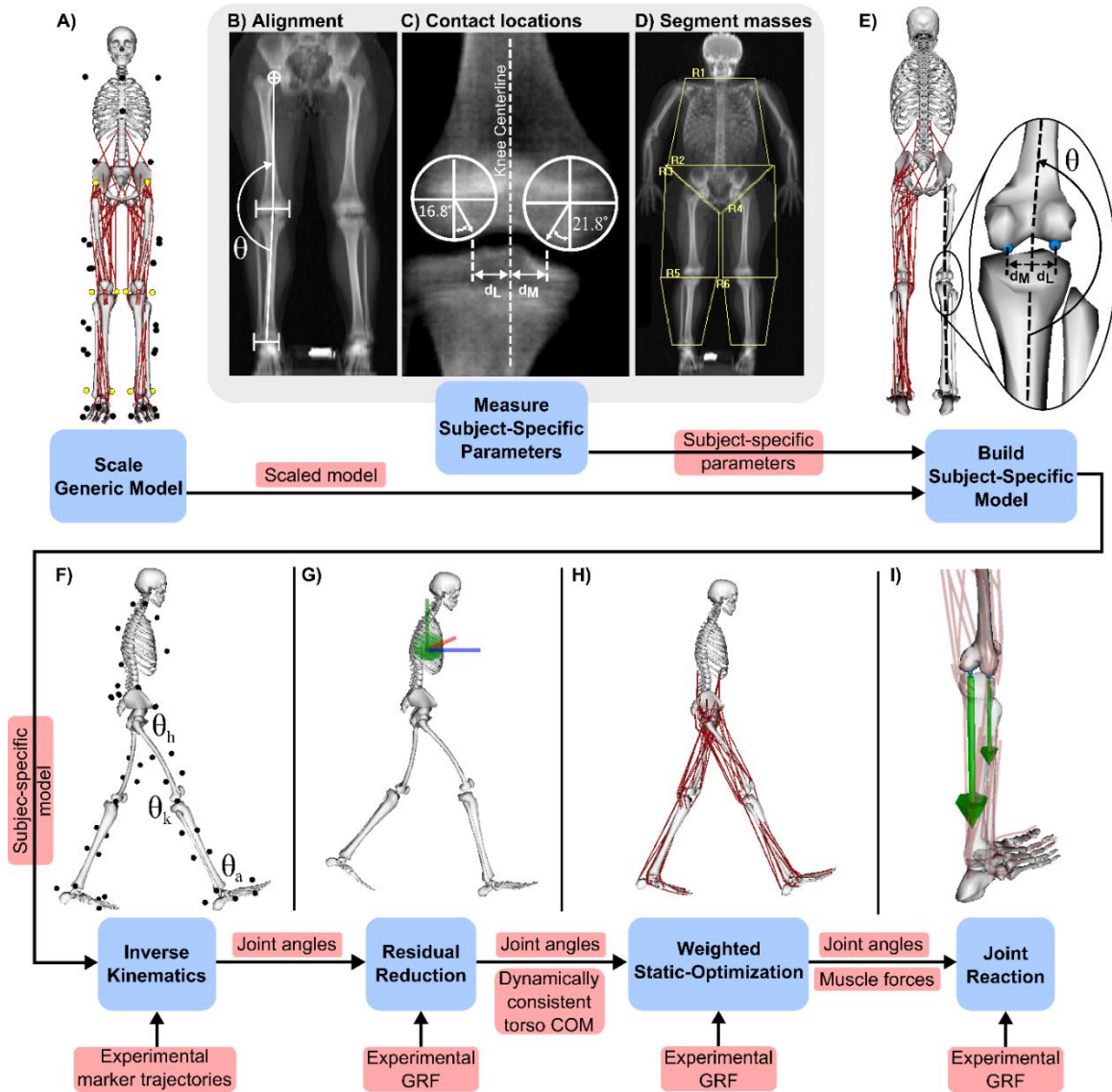


Figure 5.2 Schematic depiction of the musculoskeletal modeling workflow used to resolve medial and lateral tibiofemoral contact forces. The blue blocks represent the analysis step. The red blocks represent step outcomes and inputs. **A)** The generic musculoskeletal model is scaled for each participant using experimental markers placed on anatomical landmarks (highlighted in yellow for the lower-extremity). **B)** Anteroposterior DXA radiograph of a participant’s lower-extremity depicting how we determined subject-specific alignment for use in the musculoskeletal model. Angle θ was found by drawing lines connecting the hip, knee, and ankle joint centers, which were defined as the center of the femoral head, center of the femoral condyles, and midpoint of the medial and lateral margins of the ankle, respectively. **C)** Anteroposterior high resolution DXA radiograph of a participant’s right knee depicting how we determined the locations of the centers-of-pressure in the medial and lateral compartments. We fit a circle to each condyle and measured an angle of 21.8° toward the knee center in the medial compartment and 16.8° toward the knee center in the lateral compartment. We defined the frontal plane center-of-pressure location in each compartment as the distances (d_M and d_L) between the centerline of the knee and the location of each angle on the fitted circles. **D)** DXA image of a participant partitioned into shank, thigh, pelvis and torso segments used to specify the mass of each segment in the model. **E)** Graphic depiction of specifying subject-specific alignment (θ) and medial (d_M) and lateral (d_L) tibiofemoral contact locations. **F)** Inverse kinematics was used to determine joint angles (e.g. the hip (θ_h), knee (θ_k), and ankle (θ_a) angles) during walking. **G)** Residual reduction algorithm was used to modify the torso center of mass (COM) location (green sphere) to improve dynamic consistency. **H)** Weighted static-optimization was used to resolve muscle forces. **I)** Joint reaction analysis was used to determine medial and lateral tibiofemoral contact forces (green arrows).

We quantified each participant's lower-extremity alignment by analyzing the whole-body DXA image using established analysis methods [66]. The angle formed between the intersection of the mechanical axes of the femur and tibia was used to specify subject-specific model alignment (Figure 5.2B) [55]. To estimate subject-specific medial and lateral compartment center-of-pressure locations, we analyzed the higher resolution DXA image of each individual's right knee. We defined the center-of-pressure locations on the femoral condyles based on the approach and findings introduced by Li et al. [63] Using bi-planar fluoroscopy and 3D MRI reconstructions of the knee, Li et al. found that the *in vivo* medial-lateral locations of the centers-of-pressure, defined as the centroid of the area enclosed by the intersection of tibial and femoral cartilage layers, were concentrated on the inner portion of the medial and lateral femoral condyles rather than at their mid-lines. As done by Li et al., but with our 2D radiographs, we fit a circle to each condyle and defined the center-of-pressure locations by an angle relative to the circle's vertical midline (Figure 5.2C). These angles, which Li et al. found were not statistically different at varying levels of knee flexion, were 21.8° toward the joint center for the medial compartment and 16.8° toward the joint center for the lateral compartment [63]. The whole body DXA image was sectioned at the torso, pelvis, thigh, and shank to obtain the masses for each respective segment (Figure 5.2D). The measured lower-extremity alignment, contact locations, and segment masses were used as inputs into each subject-specific model (Figure 5.2E).

Prediction of Muscle and Joint Contact Forces

The workflow for predicting medial and lateral compartment joint contact forces is depicted in Figure 5.2 F-I. In OpenSim, we used inverse kinematics to determine segment motion by minimizing the distance between markers on the model and the experimental marker trajectories (Figure 5.2F). Next, we implemented a residual reduction algorithm [10] to refine the

torso mass properties to improve dynamic consistency between the external forces and segment accelerations (Figure 5.2G). We used a weighted static optimization approach to estimate muscle forces that satisfied the net joint torques and reproduced the measured walking motions (Figure 5.2H). As done in our validation study, the objective function minimized the sum of squared muscle activations, while incorporating individual muscle weighting constants of 1.5 for the gastrocnemius, 2 for the hamstrings, and 1 for all other muscles. Finally, we calculated the contact force in each compartment using OpenSim's joint reaction analyses [12], which determined the resultant forces and moments acting on each articulating joint structure from all muscle forces and external and inertial loads applied to the model (Figure 5.2I). The tibiofemoral contact forces in each compartment were computed as the component of each resultant force normal to the tibial plateau. We calculated the medial compartment loading rate by taking the difference between the maxima and minima of the medial compartment contact force during weight acceptance (the first 20% of the gait cycle) and dividing by the time elapsed between those extremes.

We averaged the tibiofemoral loads across three representative gait cycles for each participant. We analyzed our data at a beginning time-point (the 6th minute) and the end time-point (20th minute). The beginning time point was specified as the 6th minute rather than the 1st minute to allow for a 5 minute treadmill acclimation period.

We evaluated the dynamic consistency of our simulations by analyzing the residual forces applied to the model's center of mass. The average residuals were less than 6% BW for all participants, and there were no differences between the obese and healthy-weight group averages, which suggests that our simulations were reasonably dynamically consistent. We also qualitatively compared our predicted muscle activations to our experimental EMG data and

prior reports in the literature to ensure our predictions were physiologically representative. We found good agreement between the periods of predicted activation and EMG during early stance for the quadriceps (vasti and rectus femoris) and hamstrings (semimembranosus, semitendinosus, biceps femoris short head, and biceps femoris long head) and during mid-stance for the gastrocnemius.

Statistical Analysis

We computed group means and standard deviations for each variable. Two-factor repeated measures ANOVA tests determined how obesity and walking duration affected joint loads. When a significant main effect was observed, post hoc comparisons were made using the Tukey method, where $p < 0.05$ defined significance. Linear regression analysis was used to determine the relationship between participant anthropometrics (e.g. BMI-Z and BF%) and the medial-lateral distribution of the knee joint contact forces. We conducted a power analysis with $\alpha = 0.05$ and found power levels of $\beta \geq 0.979$ for the ANOVA tests of our primary outcome measures (i.e. absolute and normalized compartment contact forces), indicating our sample size was sufficient to detect meaningful differences [100]. SigmaPlot version 11.0 (Systat Software, Inc., San Jose, CA) was used to perform statistical analyses.

5.4 Results

Obesity affected tibiofemoral loading (Figure 5.3). In the obese vs. healthy-weight participants, peak contact forces (N) during stance were 2.1 times greater in the medial compartment ($p < 0.001$), but similar in the lateral compartment ($p = 0.406$). Normalized to BW, medial compartment contact forces were similar ($p = 0.704$), while lateral compartment contact forces were lower in the obese vs. health-weight children ($p < 0.001$). Normalized to the BMD in the medial tibial epiphysis region of interest, peak medial forces ($\text{N} \cdot \text{kg}^{-1} \cdot \text{cm}^2$) were 1.77 times

larger in the obese vs. healthy-weight individuals; no differences between groups were found for BMD normalized forces in the lateral compartment. Peak early stance knee flexion-extension angles were similar between groups ($p=0.778$), while the peak early stance knee adduction moment ($N\cdot m$) was 2.2 times greater in the obese vs. healthy-weight children ($p<0.001$).

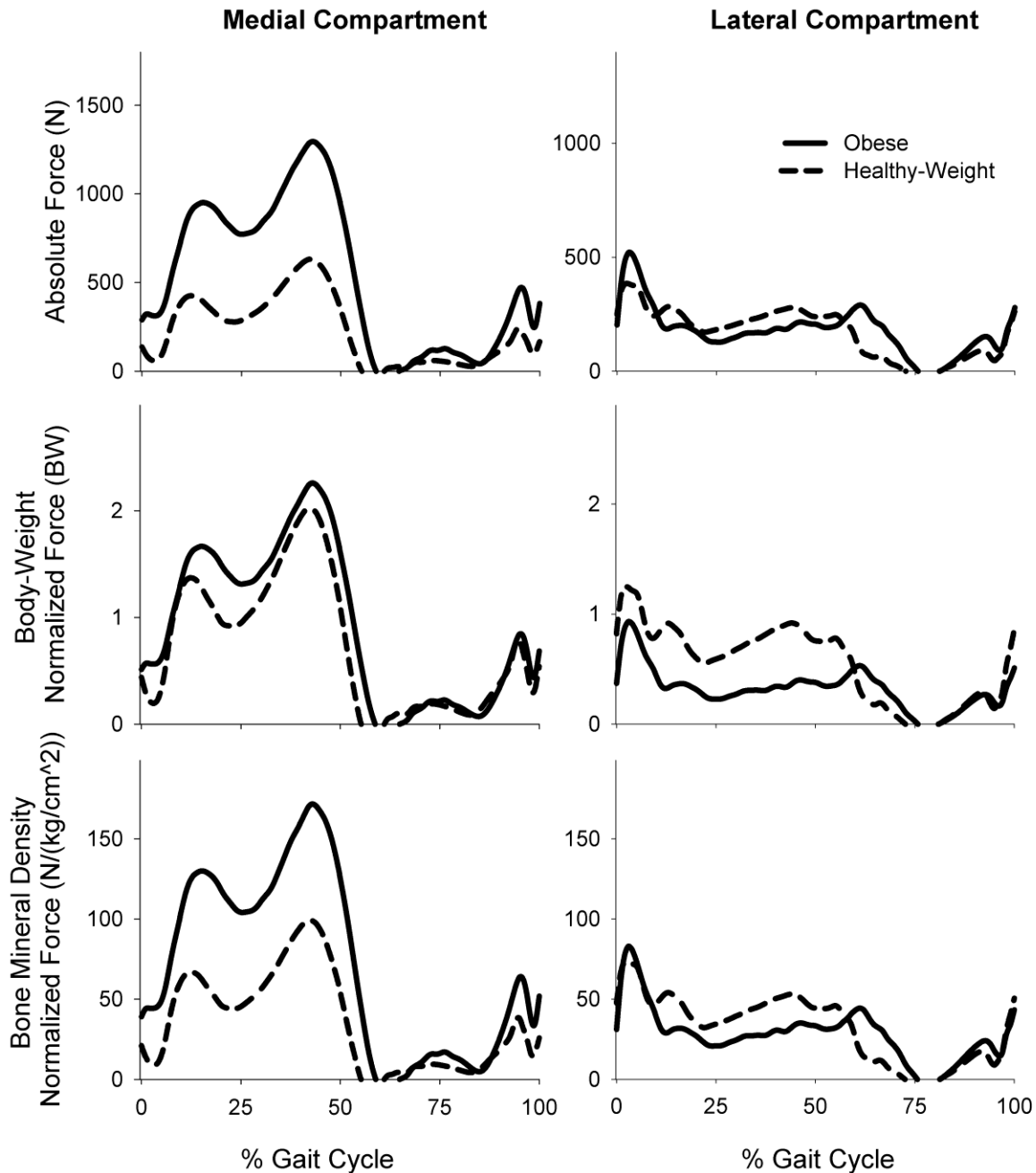


Figure 5.3 Absolute (top), BW normalized (middle) and BMD normalized (bottom) medial (left) and lateral (right) compartment contact forces in the obese (solid black line) and healthy-weight (dashed black line) participants.

The average medial-lateral distribution during stance was 22% more medially distributed in the obese (85% medial load share) vs. healthy-weight (63% medial load share) children (Figure 5.4). The medial compartment loading rate ($\text{kN}\cdot\text{s}^{-1}$) was 1.78 times greater in the obese ($5.57 \text{ kN}\cdot\text{s}$) vs. the healthy-weight ($3.12 \text{ kN}\cdot\text{s}$) participants ($p<0.001$). The medial compartment loading rate normalized to medial tibial epiphysis BMD ($\text{N}\cdot\text{kg}^{-1}\cdot\text{cm}^2\cdot\text{s}^{-1}$) was 1.53 times greater in the obese vs. the healthy-weight children ($p=0.005$).

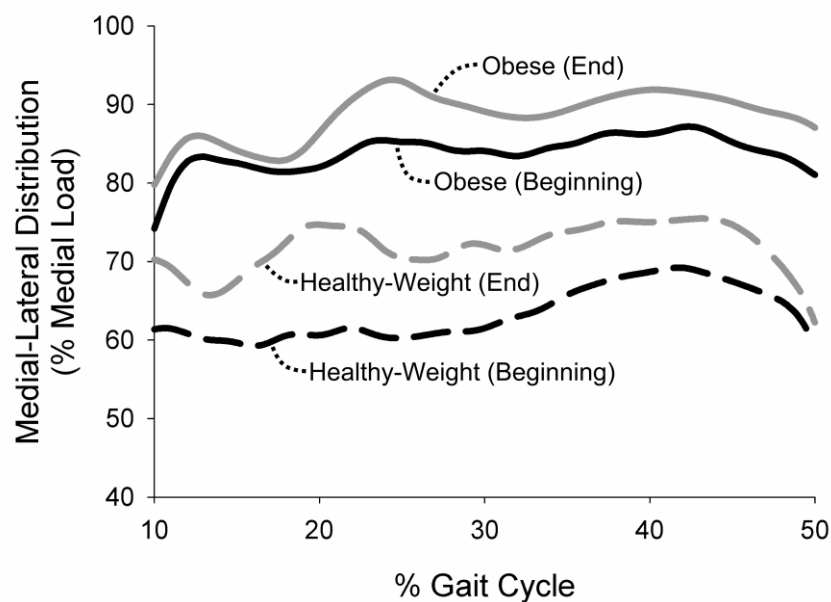


Figure 5.4 The medial-lateral distribution of the tibiofemoral contact force (% medial load) in the obese (solid lines) and healthy-weight (dashed lines) at the beginning (black lines) and end (gray lines) time-points.

Walking duration affected tibiofemoral loading. At the end vs. beginning time-point, first peak medial compartment contact forces increased by 122 N (12% increase) in the obese participants, and 65 N (15% increase) in the healthy-weight participants. The medial load share increased to 90% in the obese children and 72% in the healthy-weight children at the end time-point (Figure 5.4). The medial compartment loading rate increased 17% in both groups at the end vs. the beginning time-point ($p=0.001$). The peak early stance knee flexion-extension angle was not affected by duration in either group ($p=0.148$). The knee adduction moment increased by 2.5

N•m in the obese group ($p<0.001$) and 2.0 N•m in the healthy-weight group ($p=0.004$) at the end vs. beginning time-point.

There was a strong linear relationship ($r^2=0.79$, $p<0.001$) between body fat percentage and the medial-lateral distribution of the tibiofemoral contact forces (Figure 5.5). The relationship was described by:

$$\% \text{ Medial Load} = 1.34 \cdot \text{BF}\% + 28.27$$

There was a moderate linear relationship between BMI-Z score and the medial-lateral distribution ($r^2=0.50$, $p<0.001$). There was no relationship between the lower-extremity alignment and the medial lateral distribution ($r^2=0.01$, $p=0.917$).

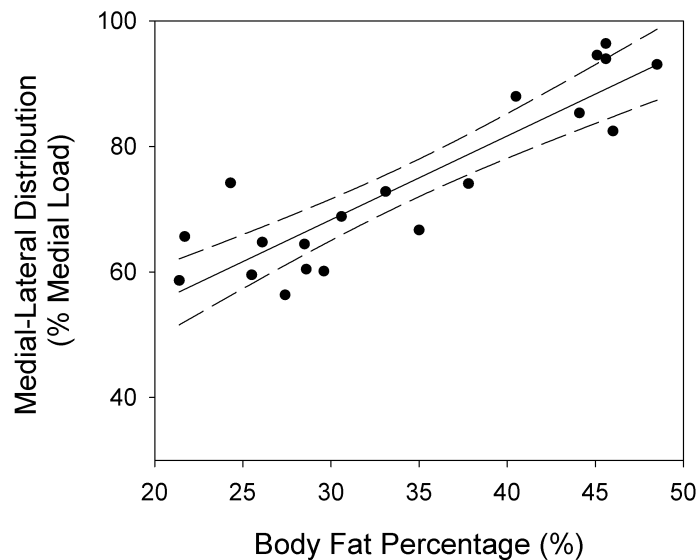


Figure 5.5 The relationship between BF% and the average medial-lateral distribution during stance. The solid line represents the linear regression and the dashed lines represent the 95% confidence intervals. The regression equation describing the relationship was $\% \text{ Medial Load} = 1.34 \cdot \text{BF}\% + 28.27$.

Muscle forces were the main contributor to the total tibiofemoral contact force (Figure 5.6). Peak early stance quadriceps muscle forces (N) were statistically similar between obese and healthy-weight children ($p=0.10$), but greater at the end vs. the beginning time-point in both groups ($p=0.023$). Peak mid to late stance quadriceps muscle forces were not affected by group

($p=0.626$) or duration ($p=0.089$). Peak gastrocnemius muscle forces were greater in the obese vs. healthy-weight children ($p=0.010$), but similar at the end vs. beginning time-points in both groups ($p=0.292$).

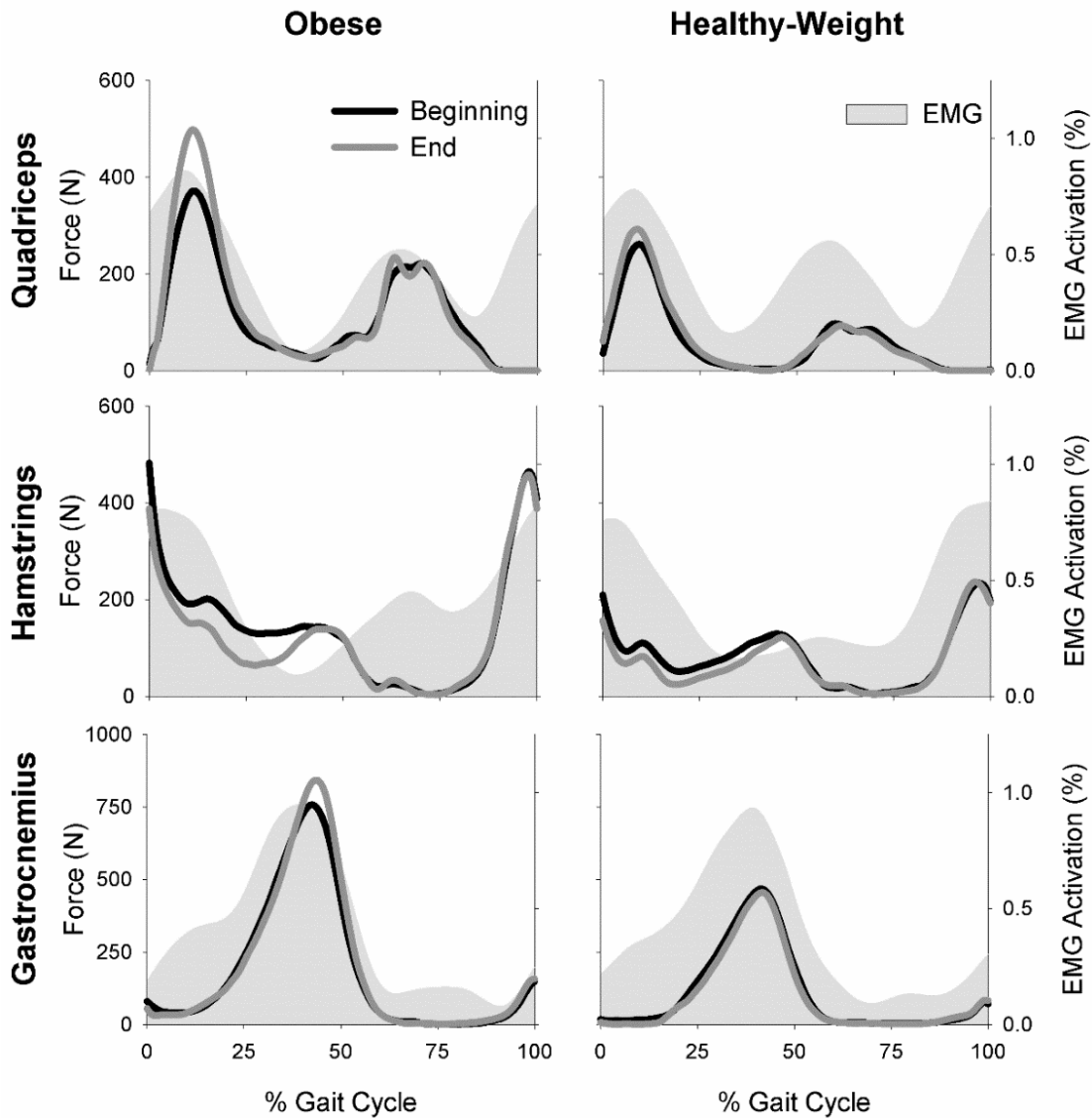


Figure 5.6 Quadriceps (vasti and rectus femoris; top), hamstrings (semimembranosus, semitendinosus, biceps femoris short-head, and biceps femoris long-head; middle), and gastrocnemius muscle forces in the obese (left panels) and healthy-weight children (right panels) at the beginning (black lines) and end (gray lines). EMG data from the vasti (vastus medialis, vastus lateralis, and rectus femoris), hamstrings (semimembranosus, and biceps femoris long-head), and gastrocnemius, normalized to the peak value during each trial and expressed as percentage are represented by the gray shading. Due to movement artifact at heel strike that persisted after signal processing, EMG data for the gastrocnemius was included for only 3 obese participants and 7 healthy-weight participants. At mid-stance, hamstring muscle force production was due to the biceps femoris short head, which was not assessed with EMG.

5.5 Discussion

The goal of this study was to evaluate how pediatric obesity and walking duration affect tibiofemoral loading. We found that obese children walk with greater medial compartment loads and had greater medial load share compared to healthy-weight children. Since lateral compartment loads were similar between groups, we only partially accept our first hypothesis. Additionally, we also found that the medial load share increased linearly with BF%. In both groups, walking duration altered the tibiofemoral contact forces by increasing the medial load share, the peak medial compartment forces, and the medial compartment loading rate. Since the obese children had similar changes due to duration compared to the healthy-weight children, we only partially accept our second hypothesis.

We found good agreement between our predictions of the medial-lateral distribution in our healthy-weight participants (63% medial load share) compared to measurements obtained during walking from instrumented knee implants in adults with similar lower-extremity alignment [53]. Our finding of elevated absolute knee adduction moments and elevated absolute, but similar BW normalized medial compartment forces in our obese participants is consistent with reported greater absolute, but similar BW normalized knee adduction moments in obese vs. healthy-weight children [4, 6]. In contrast, McMillan et al. reported lower BW normalized knee adduction moments in obese vs. healthy-weight children [74]. The finding of statistically similar quadriceps muscle forces but greater gastrocnemius muscle forces in the obese vs. healthy-weight children in this study is consistent with our findings from a previous muscle function study [9]. The similar sagittal plane knee angles between groups in this study is similar to findings from Shultz et al. [6], but different to findings from Gushue et al. [4]. These discrepancies in the literature are likely due to differences in experimental methodologies, such

as kinematic marker sets, walking speed, as well as differences in participant characteristics like severity of overweight and obesity, gender, age, and leg length. In this regard, our study had several strengths: our participant's had similar age, gender, and leg length; walking speed was standardized; and we used radiographic measures in conjunction with a robust kinematic marker set that was specifically designed for use in obese individuals to accurately track segment motion in all three planes [7]. Therefore, we are confident that the kinematic and kinetic results reported in this present study are representative.

Walking duration increased medial loading in both groups. Since a greater imbalance of the medial-lateral distribution at the knee is associated with negative orthopedic outcomes, this finding suggests that longer durations of walking may increase the possibility of bone and joint tissue injuries in all children at risk for musculoskeletal injury. While walking duration affected loading in both groups, the baseline values for medial loads/loading rates in the obese children were significantly higher. Therefore, longer activity durations may increase musculoskeletal injury risk more in the obese children compared to the healthy-weight children. It may be advantageous for obese children suffering from knee pain or with a history of knee pathology to engage in shorter (e.g. <20 minute) bouts of activity. However, knee joint loads incurred during walking may be smaller compared to joint loads during more vigorous forms of activity (e.g. running) and walking physical activity may have a limited impact on orthopedic outcomes. Future studies that examine the relationship between walking physical activity and lower extremity musculoskeletal injury in obese children are needed to address this issue.

Of the tested variables, we found that BF% was the best predictor of the medial load share ($r^2=0.79$). BF% explained a greater proportion of the medial load share variance than BMI ($r^2=0.50$). Combined with our previous finding of stronger relationships between muscle forces

and gait kinematics and BF% compared to BMI during walking in children [9], these results indicate that there may be gait adaptations in children with higher levels of BF% that contributes to altered knee loading. This suggests that a reduction in BF% likely improves the distribution of knee loads and that some benefit would remain if obese children maintain the same weight but increase muscle mass due to strengthening. The relationships between the medial load share and both BF% and BMI may partially explain the previously reported positive association between pediatric obesity and knee pain [89].

During the adolescent growth spurt there is a disassociation between longitudinal bone growth and mineral accrual, which affects bone quality and microarchitecture [101]. This imbalance, combined with findings that obese children have low bone mass and area for their weight [102], suggests that larger and/or abnormally distributed tibiofemoral contact forces during daily physical activity in obese children may play a role in the development of skeletal disorders. In order to investigate how obesity affects joint loads relative to skeletal structure, we normalized the medial contact force to the BMD in the medial tibial epiphysis ROI. While the BMD in the medial ROI was greater in the obese children, the medial contact force normalized to the BMD in the medial region was still significantly higher (1.77 times greater) in the obese vs. healthy-weight children. When considering bone adaptation to loading, the entire loading history must be considered. Therefore, a possible explanation for this imbalance (greater loads relative to BMD in the obese children) is that obese children are less physically active than their healthy-weight counterparts [103], which would result in reduced BMD [94]. Our results supports the theory that higher levels of stress on growing bones and joints in obese children when they are physically active may contribute to the increased risk of developing orthopedic disorders of the knee [101].

A limitation of the cross sectional design of this study was that we were unable to establish cause-effect relationships. Future studies should investigate knee loading and the progression of skeletal and joint development longitudinally throughout childhood. Still, our results support the theory that pediatric obesity may lead to a cycle of weight gain due to an increased risk of knee pain/pathology that may limit the ability of a child to engage in sufficient physical activity [2].

Predictions of medial and lateral tibiofemoral contact forces during walking rely on accurate estimates of muscle forces and tibiofemoral skeletal geometry [8, 50]. In a previous validation study, we demonstrated the ability of our approach to accurately predict medial and lateral contact forces during walking when using weighted-static optimization to predict muscle forces and an anterior-posterior radiograph to specify tibiofemoral alignment and contact locations [8]. For this study of biological knees, we did not assume that contact was concentrated at the center of each compartment, which appears to be unsupported in the literature. Instead, we specified the contact locations based on findings from Li et al., who demonstrated that the centers-of-pressure in each compartment occurs closer to the tibial eminence than compartment mid-line. While defining different muscle weighting factors and compartment contact locations may change the magnitudes of the contact force predictions, prior sensitivity analyses [8, 12] suggest that the relative differences due to obesity and walking duration would remain so long as the same approach is applied to each group and condition. Therefore, we believe the primary conclusions of this study are insensitive to these parameters.

5.6 Conclusion

This study demonstrated that obese children have altered knee joint loading compared to their healthy-weight counterparts. Medial compartment loading increased linearly with BF%, and

both absolute and BMD normalized medial compartment contact forces were greater in the obese children. Walking duration increased medial compartment loading in both groups. Altered tibiofemoral loading during walking in obese children may contribute to their increased risk of lower-extremity pain and pathology. Longer walking durations may increase these risks.

6. CONCLUSION

6.1 Dissertation Summary

The overarching objective of this dissertation was to better understand how pediatric obesity affects musculoskeletal function and biomechanical loading during walking. The rationale for the work of this dissertation was that the research outcomes should aid the ability of clinicians to develop effective weight-bearing physical activity interventions for the children who need it most. This dissertation has enhanced our understanding of the altered gait mechanics exhibited by obese children and allows for an improved evaluation of the long-term risk/benefit ratio of walking physical activity on the musculoskeletal system.

This dissertation had four main goals. The first goal of this dissertation was to develop a kinematic marker set and methodology that was suitable for use in obese individuals. In the first study (Chapter 2), we developed an experimental protocol that accounted for excess subcutaneous adiposity at the pelvis and determined the effect of using such a methodology to estimate muscle and joint contact forces during walking. The results of this study demonstrated the need for biomechanists to account for subcutaneous adiposity during kinematic data collection in obese individuals.

The second goal of this dissertation was to develop an experimental protocol and musculoskeletal model that addresses subject-specific tibiofemoral alignment and contact locations and computes medial and lateral compartment contact forces during walking. In the second study (Chapter 3), we created a novel knee mechanism in OpenSim that was able to incorporate subject-specific knee parameters and predict medial and lateral tibiofemoral compartment contact forces. Using data from an individual with an instrumented knee implant,

we found that our model was able to accurately predict medial and lateral tibiofemoral contact forces when we specified tibiofemoral alignment and contact locations from an anterior-posterior radiograph.

The third goal of this dissertation was to investigate the relationship between adiposity and lower extremity kinematics, muscle forces, and individual muscle contributions to the acceleration of center of mass. In the third study (Chapter 4), we evaluated how pediatric obesity affects the requirements of individual muscles during walking. The results of this study indicated that the altered gait mechanics exhibited by obese children may be attributed to greater force requirements for the hip abductor muscles.

The fourth goal of this dissertation was to determine the effects of pediatric obesity and walking duration on medial and lateral tibiofemoral contact forces. In the fourth study (Chapter 5), we applied both the experimental and computational methodologies developed in this dissertation's first two studies, and estimated tibiofemoral contact forces during walking from subject-specific musculoskeletal models. The elevated medial compartment loading during walking in obese children may contribute to the increased prevalence of tibiofemoral pain and pathology associated with pediatric obesity.

6.2 Future Work

Additional research may improve our understanding of the biomechanical mechanisms responsible for the orthopedic and locomotor disabilities caused by pediatric obesity. A limitation of the studies presented in this dissertation were that they were cross sectional by design. Therefore, we were unable to establish any cause-effect relationships in regards to the development of the musculoskeletal disabilities associated with pediatric obesity. Future studies should determine how the neuromuscular and musculoskeletal systems adapt to excess adiposity

longitudinally throughout childhood. We hope the methodological tools and techniques presented in the first two studies of this dissertation combined with the experimental results presented in the third and fourth studies of this dissertation will provide a strong foundation from which biomechanists can evaluate the impact of future longitudinal and intervention based studies aimed at improving musculoskeletal function and health in obese children.

In order to break the cycle of weight gain in pediatric obesity, clinicians and researchers may apply the knowledge gained from this dissertation to design improved guidelines for rehabilitation and physical activity. For example, in Chapter 4 we identified several specific muscles that could be targeted for strengthening and may improve walking performance in children with high levels of adiposity. Future studies should evaluate the impact of targeted muscle strengthening on the biomechanics of walking in pediatric obesity. Further, our results from Chapter 5, which describes the effects of pediatric obesity and walking duration on tibiofemoral loading, may allow clinicians to weigh the long-term risk/benefit ratio of increased physical activity on the musculoskeletal system. We found that longer activity durations may increase the risk of musculoskeletal pain and pathology of the knee. Future studies should evaluate the impact of activity quantity and duration on weight status, and musculoskeletal and cardiovascular health in children.

The development of new and/or improved experimental and computational biomechanical methods may improve our understanding of how obesity affects the neuromuscular and musculoskeletal systems. Future studies should combine measures of both mechanical and metabolic factors (e.g. cartilage health and joint biomarkers) to improve our understanding of the mechanisms by which obesity affects the development, maintenance, and degeneration of weight-bearing joints. The use of predictive musculoskeletal simulations, while

exceptionally challenging, may provide researchers with the ability to critically evaluate novel movement patterns that are efficacious for musculoskeletal health in obese children.

REFERENCES

1. Chan, G. and C.T. Chen, *Musculoskeletal effects of obesity*. Current opinion in pediatrics, 2009. 21(1): p. 65-70.
2. Smith, S., B. Sumar, and K. Dixon, *Musculoskeletal pain in overweight and obese children*. International Journal of Obesity, 2014. 38(1): p. 11-15.
3. McGraw, B., et al., *Gait and postural stability in obese and nonobese prepubertal boys*. Archives of Physical Medicine and Rehabilitation, 2000. 81(4): p. 484-489.
4. Gushue, D.L., J. Houck, and A.L. Lerner, *Effects of childhood obesity on three-dimensional knee joint biomechanics during walking*. J Pediatr Orthop, 2005. 25(6): p. 763-8.
5. McMillan, A.G., et al., *Frontal plane lower extremity biomechanics during walking in boys who are overweight versus healthy weight*. Pediatric Physical Therapy, 2009. 21(2): p. 187-193.
6. Shultz, S.P., et al., *Effects of pediatric obesity on joint kinematics and kinetics during 2 walking cadences*. Archives of physical medicine and rehabilitation, 2009. 90(12): p. 2146-2154.
7. Lerner, Z.F., W.J. Board, and R.C. Browning, *Effects of an Obesity-Specific Marker Set on Estimated Muscle/Joint Forces in Walking*. Medicine and Science in Sports and Exercise, 2013.
8. Lerner, Z.F., et al., *How tibiofemoral alignment and contact locations affect predictions of medial and lateral tibiofemoral contact forces*. Journal of Biomechanics, 2015. 48(0): p. 644-50.

9. Lerner, Z.F., et al., *Does adiposity affect muscle function during walking in children?* Journal of Biomechanics, 2014. 47(12): p. 2975-2982.
10. Delp, S.L., et al., *OpenSim: open-source software to create and analyze dynamic simulations of movement.* IEEE Trans Biomed Eng, 2007. 54(11): p. 1940-50.
11. Delp, S.L., et al., *Hamstrings and psoas lengths during normal and crouch gait: implications for muscle-tendon surgery.* J Orthop Res, 1996. 14(1): p. 144-51.
12. Steele, K.M., et al., *Compressive tibiofemoral force during crouch gait.* Gait & Posture, 2012. 35(4): p. 556-560.
13. Correa, T.A., et al., *Contributions of individual muscles to hip joint contact force in normal walking.* Journal of Biomechanics, 2010. 43(8): p. 1618-1622.
14. Shelburne, K.B., et al., *Effects of foot orthoses and valgus bracing on the knee adduction moment and medial joint load during gait.* Clin Biomech (Bristol, Avon), 2008. 23(6): p. 814-21.
15. Peters, A., et al., *Quantification of soft tissue artifact in lower limb human motion analysis: A systematic review.* Gait & Posture, 2010. 31(1): p. 1-8.
16. Mokdad, A.H., et al., *The continuing epidemics of obesity and diabetes in the United States.* JAMA, 2001. 286(10): p. 1195-200.
17. DeVita, P. and T. Hortobagyi, *Obesity is not associated with increased knee joint torque and power during level walking.* J Biomech, 2003. 36: p. 1355-1362.
18. Lai, P.P., et al., *Three-dimensional gait analysis of obese adults.* Clin Biomech (Bristol, Avon), 2008. 23 Suppl 1: p. S2-6.

19. Spyropoulos, P., et al., *Biomechanical gait analysis in obese men*. Archives of physical medicine and rehabilitation, 1991. 72(13): p. 1065.
20. Kadaba, M.P., H.K. Ramakrishnan, and M.E. Wootten, *Measurement of lower extremity kinematics during level walking*. Journal of Orthopaedic Research, 1990. 8(3): p. 383-392.
21. Cappozzo, A., et al., *Position and orientation in space of bones during movement: anatomical frame definition and determination*. Clinical Biomechanics, 1995. 10(4): p. 171-178.
22. Browning, R.C. and R. Kram, *Effects of obesity on the biomechanics of walking at different speeds*. Med Sci Sports Exerc, 2007. 39(9): p. 1632-41.
23. Ganley, K.J. and C.M. Powers, *Determination of lower extremity anthropometric parameters using dual energy X-ray absorptiometry: the influence on net joint moments during gait*. Clin Biomech (Bristol, Avon), 2004. 19(1): p. 50-6.
24. Ehlen, K., R. Reiser, and R. Browning, *Biomechanics And Energetics Of Walking Uphill: A Better Form Of Exercise For Obese Adults?* Med Sci Sports Exerc, 2010. 42(5): p. 133-133.
25. You, B.M., et al., *In vivo measurement of 3-D skeletal kinematics from sequences of biplane radiographs: Application to knee kinematics*. Medical Imaging, IEEE Transactions on, 2001. 20(6): p. 514-525.
26. Piazza, S.J., et al., *Assessment of the functional method of hip joint center location subject to reduced range of hip motion*. Journal of Biomechanics, 2004. 37(3): p. 349-356.

27. Stagni, R., et al., *Effects of hip joint centre mislocation on gait analysis results*. Journal of Biomechanics, 2000. 33(11): p. 1479-1487.
28. Merletti, R., *Standard for Reporting EMG data*. J Electromyogr Kinesiol, 1999. 9: p. III-IV.
29. Lerner, Z.F., et al., *The Effects of Walking Speed on Tibiofemoral Loading Estimated Via Musculoskeletal Modeling*. J Appl Biomech, 2013.
30. Yamaguchi, G.T. and F.E. Zajac, *A planar model of the knee joint to characterize the knee extensor mechanism*. Journal of Biomechanics, 1989. 22(1).
31. Delp, S.L., et al., *An interactive graphics-based model of the lower extremity to study orthopaedic surgical procedures*. IEEE Trans Biomed Eng, 1990. 37(8): p. 757-67.
32. Fregly, B.J., et al., *Grand challenge competition to predict in vivo knee loads*. Journal of Orthopaedic Research, 2012. 30(4): p. 503-513.
33. Collins, T.D., et al., *A six degrees-of-freedom marker set for gait analysis: Repeatability and comparison with a modified Helen Hayes set*. Gait & Posture, 2009. 30(2): p. 173-180.
34. Heller, M.O., et al., *Musculo-skeletal loading conditions at the hip during walking and stair climbing*. Journal of Biomechanics, 2001. 34(7): p. 883-893.
35. Zhao, D., et al., *Correlation between the knee adduction torque and medial contact force for a variety of gait patterns*. Journal of Orthopaedic Research, 2007. 25(6): p. 789-797.
36. Minetto, M.A., et al., *Feasibility study of detecting surface electromyograms in severely obese patients*. Journal of Electromyography and Kinesiology, 2013. 23(2): p. 285-295.
37. Browning, R.C., et al., *Effects of obesity and sex on the energetic cost and preferred speed of walking*. J Appl Physiol, 2006. 100(2): p. 390-8.

38. Rao, G., et al., *Influence of body segments' parameters estimation models on inverse dynamics solutions during gait*. Journal of Biomechanics, 2006. 39(8): p. 1531-1536.
39. Sharma, L., et al., *Knee adduction moment, serum hyaluronan level, and disease severity in medial tibiofemoral osteoarthritis*. Arthritis Rheum, 1998. 41: p. 1233-40.
40. Dillon, C.F., et al., *Prevalence of knee osteoarthritis in the United States: arthritis data from the Third National Health and Nutrition Examination Survey 1991-94*. The Journal of Rheumatology, 2006. 33(11): p. 2271-2279.
41. Sharma, L., et al., *The role of knee alignment in disease progression and functional decline in knee osteoarthritis*. JAMA: the journal of the American Medical Association, 2001. 286(2): p. 188-195.
42. Ritter, M.A., et al., *Postoperative alignment of total knee replacement. Its effect on survival*. Clin Orthop Relat Res, 1994(299): p. 153-6.
43. Morrison, J.B., *The mechanics of the knee joint in relation to normal walking*. J Biomech, 1970. 3(1): p. 51-61.
44. Hast, M.W. and S.J. Piazza, *Dual-joint modeling for estimation of total knee replacement contact forces during locomotion*. J Biomech Eng, 2013. 135(2): p. 021013.
45. Lin, Y.-C., et al., *Simultaneous prediction of muscle and contact forces in the knee during gait*. Journal of biomechanics, 2010. 43(5): p. 945-952.
46. Bei, Y. and B.J. Fregly, *Multibody dynamic simulation of knee contact mechanics*. Medical engineering & physics, 2004. 26(9): p. 777-789.

47. Yang, N.H., et al., *Effect of frontal plane tibiofemoral angle on the stress and strain at the knee cartilage during the stance phase of gait*. Journal of Orthopaedic Research, 2010. 28(12): p. 1539-1547.
48. Thelen, D.G., K.W. Choi, and A.M. Schmitz, *Co-Simulation of Neuromuscular Dynamics and Knee Mechanics During Human Walking*. Journal of biomechanical engineering, 2014. 136(2): p. 021033.
49. Kumar, D., K.S. Rudolph, and K.T. Manal, *EMG-driven modeling approach to muscle force and joint load estimations: Case study in knee osteoarthritis*. Journal of Orthopaedic Research, 2012. 30(3): p. 377-383.
50. Gerus, P., et al., *Subject-specific knee joint geometry improves predictions of medial tibiofemoral contact forces*. J Biomech, 2013. 46(16): p. 2778-86.
51. Winby, C.R., et al., *Muscle and external load contribution to knee joint contact loads during normal gait*. Journal of Biomechanics, 2009. 42(14): p. 2294-2300.
52. Hurwitz, D.E., et al., *The knee adduction moment during gait in subjects with knee osteoarthritis is more closely correlated with static alignment than radiographic disease severity, toe out angle and pain*. Journal of Orthopaedic Research, 2002. 20(1): p. 101-107.
53. Halder, A., et al., *Influence of limb alignment on mediolateral loading in total knee replacement: in vivo measurements in five patients*. J Bone Joint Surg Am, 2012. 94(11): p. 1023-9.
54. Hsu, R.W., et al., *Normal axial alignment of the lower extremity and load-bearing distribution at the knee*. Clin Orthop Relat Res, 1990(255): p. 215-27.

55. Moreland, J.R., L.W. Bassett, and G.J. Hanker, *Radiographic analysis of the axial alignment of the lower extremity*. The Journal of Bone & Joint Surgery, 1987. 69(5): p. 745-749.
56. DeMers, M.S., S. Pal, and S.L. Delp, *Changes in tibiofemoral forces due to variations in muscle activity during walking*. Journal of Orthopaedic Research, 2014. 32(6): p. 769-776.
57. Meyer, A.J., et al. *Evaluation of Regression Equations for Medial and Lateral Contact Force From Instrumented Knee Implant Data*. in *ASME 2011 Summer Bioengineering Conference*. 2011. American Society of Mechanical Engineers.
58. Zhao, D., et al., *In vivo medial and lateral tibial loads during dynamic and high flexion activities*. Journal of Orthopaedic Research, 2007. 25(5): p. 593-602.
59. Herzog, W., D. Longino, and A. Clark, *The role of muscles in joint adaptation and degeneration*. Langenbeck's Archives of Surgery, 2003. 388(5): p. 305-315.
60. Schmitz, A., et al., *Differences in lower-extremity muscular activation during walking between healthy older and young adults*. Journal of Electromyography and Kinesiology, 2009. 19(6): p. 1085-1091.
61. B athis, H., et al., *Alignment in total knee arthroplasty: A COMPARISON OF COMPUTER-ASSISTED SURGERY WITH THE CONVENTIONAL TECHNIQUE*. Journal of Bone & Joint Surgery, British Volume, 2004. 86-B(5): p. 682-687.
62. Cooke, D., et al., *Axial lower-limb alignment: comparison of knee geometry in normal volunteers and osteoarthritis patients*. Osteoarthritis and Cartilage, 1997. 5(1): p. 39-47.

63. Li, G., et al., *In Vivo Articular Cartilage Contact Kinematics of the Knee: An Investigation Using Dual-Orthogonal Fluoroscopy and Magnetic Resonance Image-Based Computer Models*. The American Journal of Sports Medicine, 2005. 33(1): p. 102-107.
64. Shultz, S.P., et al., *Childhood obesity and walking: guidelines and challenges*. Int J Pediatr Obes, 2011. 6(5-6): p. 332-41.
65. Maffels, C., et al., *Energy expenditure during walking and running in obese and nonobese prepubertal children*. The Journal of Pediatrics, 1993. 123(2): p. 193-199.
66. Taylor, E.D., et al., *Orthopedic complications of overweight in children and adolescents*. Pediatrics, 2006. 117(6): p. 2167-74.
67. Wearing, S.C., et al., *The impact of childhood obesity on musculoskeletal form*. Obes Rev, 2006. 7(2): p. 209-18.
68. Zabinski, M.F., et al., *Overweight Children's Barriers to and Support for Physical Activity*. Obesity Research, 2003. 11(2): p. 238-246.
69. Daniels, S.R., P.R. Khoury, and J.A. Morrison, *The Utility of Body Mass Index as a Measure of Body Fatness in Children and Adolescents: Differences by Race and Gender*. Pediatrics, 1997. 99(6): p. 804-807.
70. Blimkie, C.R., D. Sale, and O. Bar-Or, *Voluntary strength, evoked twitch contractile properties and motor unit activation of knee extensors in obese and non-obese adolescent males*. European Journal of Applied Physiology and Occupational Physiology, 1990. 61(3-4): p. 313-318.
71. Shultz, S.P., et al., *Body size and walking cadence affect lower extremity joint power in children's gait*. Gait & Posture, 2010. 32(2): p. 248-252.

72. Tsiros, M., et al., *Knee extensor strength differences in obese and healthy-weight 10-to 13-year-olds*. *European Journal of Applied Physiology*, 2013. 113(6): p. 1415-1422.
73. van der Krogt, M.M., S.L. Delp, and M.H. Schwartz, *How robust is human gait to muscle weakness?* *Gait & Posture*, 2012. 36(1): p. 113-119.
74. McMillan, A.G., et al., *Sagittal and frontal plane joint mechanics throughout the stance phase of walking in adolescents who are obese*. *Gait Posture*, 2010. 32(2): p. 263-8.
75. Anderson, F.C. and M.G. Pandy, *Individual muscle contributions to support in normal walking*. *Gait and Posture*, 2003. 17: p. 159-169.
76. Lin, Y.-C., H.J. Kim, and M.G. Pandy, *A computationally efficient method for assessing muscle function during human locomotion*. *International Journal for Numerical Methods in Biomedical Engineering*, 2011. 27(3): p. 436-449.
77. Taylor, R., *Interpretation of the correlation coefficient: a basic review*. *Journal of diagnostic medical sonography*, 1990. 6(1): p. 35-39.
78. Blakemore, V.J., et al., *Mass affects lower extremity muscle activity patterns in children's gait*. *Gait & Posture*, 2013. 38(4): p. 609-613.
79. Hof, A.L., *Scaling gait data to body size*. *Gait & Posture*, 1996. 4(3): p. 222-223.
80. Dorn, T.W., Y.-C. Lin, and M.G. Pandy, *Estimates of muscle function in human gait depend on how foot-ground contact is modelled*. *Computer Methods in Biomechanics and Biomedical Engineering*, 2011. 15(6): p. 657-668.
81. Rutherford, D.J. and C. Hubble-Kozey, *Explaining the hip adduction moment variability during gait: Implications for hip abductor strengthening*. *Clinical Biomechanics*, 2009. 24(3): p. 267-273.

82. Shiavi, R., et al., *Normative childhood EMG gait patterns*. J Orthop Res, 1987. 5(2): p. 283-95.
83. Steele, K.M., et al., *Muscle contributions to vertical and fore-aft accelerations are altered in subjects with crouch gait*. Gait & posture, 2013. 38(1): p. 86-91.
84. Liu, M.Q., et al., *Muscle contributions to support and progression over a range of walking speeds*. J Biomech, 2008. 41(15): p. 3243-52.
85. John, C.T., et al., *Contributions of muscles to mediolateral ground reaction force over a range of walking speeds*. J Biomech, 2012. 45(14): p. 2438-43.
86. Borghese, N.A., L. Bianchi, and F. Lacquaniti, *Kinematic determinants of human locomotion*. Journal of Physiology, 1996. 494(3): p. 863-879.
87. Hubley-Kozey, C.L., et al., *Neuromuscular alterations during walking in persons with moderate knee osteoarthritis*. Journal of Electromyography and Kinesiology, 2006. 16(4): p. 365-378.
88. Gribble, P.A. and J. Hertel, *Effect of hip and ankle muscle fatigue on unipedal postural control*. Journal of Electromyography and Kinesiology, 2004. 14(6): p. 641-646.
89. Stovitz, S.D., et al., *Musculoskeletal pain in obese children and adolescents*. Acta Pædiatrica, 2008. 97(4): p. 489-493.
90. Lerner, Z.F., W.J. Board, and R.C. Browning, *Effects of obesity on lower extremity muscle function during walking at two speeds*. Gait Posture, 2013.
91. Maffiuletti, N.A., et al., *The Impact of Obesity on In Vivo Human Skeletal Muscle Function*. Current Obesity Reports, 2013. 2(3): p. 251-260.

92. Maffiuletti, N., et al., *Quadriceps muscle function characteristics in severely obese and nonobese adolescents*. European Journal of Applied Physiology, 2008. 103(4): p. 481-484.
93. Jones, G., K. Bennell, and F.M. Cicuttini, *Effect of physical activity on cartilage development in healthy kids*. British journal of sports medicine, 2003. 37(5): p. 382-383.
94. Hind, K. and M. Burrows, *Weight-bearing exercise and bone mineral accrual in children and adolescents: A review of controlled trials*. Bone, 2007. 40(1): p. 14-27.
95. Davids, J.R., M. Huskamp, and A.M. Bagley, *A Dynamic Biomechanical Analysis of the Etiology of Adolescent Tibia Vara*. Journal of Pediatric Orthopaedics, 1996. 16(4): p. 461-468.
96. Wittmeier, K.D.M., R.C. Mollard, and D.J. Kriellaars, *Physical Activity Intensity and Risk of Overweight and Adiposity in Children*. Obesity, 2008. 16(2): p. 415-420.
97. Woolf-May, K., et al., *The efficacy of accumulated short bouts versus single daily bouts of brisk walking in improving aerobic fitness and blood lipid profiles*. Health Educ Res, 1999. 14(6): p. 803-15.
98. Lo, G.H., et al., *Cross-sectional DXA and MR measures of tibial periarticular bone associate with radiographic knee osteoarthritis severity*. Osteoarthritis Cartilage, 2012. 20(7): p. 686-93.
99. Anderson, F.C. and M.G. Pandy, *A Dynamic Optimization Solution for Vertical Jumping in Three Dimensions*. Comput Methods Biomech Biomed Engin, 1999. 2(3): p. 201-231.
100. Cohen, J., *A power primer*. Psychological Bulliten, 1992. 112: p. 155-159.

101. Wills, M., *Orthopedic complications of childhood obesity*. *Pediatric physical therapy*, 2004. 16(4): p. 230-235.
102. Goulding, A., et al., *Overweight and obese children have low bone mass and area for their weight*. *Int J Obes Relat Metab Disord*, 2000. 24(5): p. 627-32.
103. Trost, S.G., et al., *Physical activity and determinants of physical activity in obese and non-obese children*. *International Journal of Obesity*, 2001. 25(6): p. 822-829.